U.S.G.S. Award Number: G10AP00006
Project Dates: 12/01/09 – 11/30/10

iShake: Using Personal Devices to Deliver Rapid Semi-Qualitative Earthquake Shaking Information

Shideh Dashti[1], Jack Reilly[2], Jonathan D. Bray[3], Alex Bayen[4], Steven Glaser[5], and Ervasti Mari[6]

[1]Post Doctoral Scholar, [2]Graduate Student Researcher, [3]Professor, [4]Associate Professor, [5]Professor, and [6]Visiting Scholar Student

Principal Investigators:
Professors Jonathan D. Bray, Alex Bayen, and Steven Glaser
Department of Civil and Environmental Engineering
University of California, Berkeley
453 Davis Hall, MC-1710
Berkeley, CA 94720-1710
Tel. (510) 642-9843
Fax. (510) 642-7476
bray@ce.berkeley.edu
URL: http://www.ce.berkeley.edu/~bray/

Final Technical Report

February 28, 2011

U.S.G.S. Award Number: G10AP00006

iShake: Using Personal Devices to Deliver Rapid Semi-Qualitative Earthquake Shaking Information

Shideh Dashti, Jack Reilly, Jonathan D. Bray, Alex Bayen, Steven Glaser, and Ervasti Mari
University of California, Berkeley

ABSTRACT

Emergency responders must "see" the effects of an earthquake clearly and rapidly so that they can respond effectively to the damage it has produced. Great strides have been made recently in developing methodologies that deliver rapid and accurate post-earthquake information. However, shortcomings still exist. The iShake project is an innovative use of cell phones and information technology to bridge the gap between the high quality, but sparse, ground motion instrument data that are used to help develop ShakeMap and the low quality, but large quantity, human observational data collected to construct a "Did You Feel It?" (DYFI)-based map.

Rather than using people as measurement "devices" as is being done through DYFI, the iShake project is using their cell phones to measure ground motion intensity parameters and automatically deliver the data to the U.S. Geological Survey (USGS) for processing and dissemination. In this participatory sensing paradigm, quantitative shaking data from numerous cellular phones will enable the USGS to produce shaking intensity maps more accurately than presently possible.

The phone sensor, however, is an imperfect device with performance variations among phones of a given model as well as between models. The sensor is the entire phone, not just the micro-machined transducer inside. A series of 1-D and 3-D shaking table tests were performed at UC San Diego and UC Berkeley, respectively, to evaluate the performance of a class of cell phones. In these tests, seven iPhones and iPod Touch devices that were mounted at different orientations were subjected to 124 earthquake ground motions to characterize their response and reliability as seismic sensors. The testing also provided insight into the seismic response of unsecured and falling instruments.

Pilot software has been developed that captured the measured data during the shaking table tests. The data are sent automatically as a text message immediately after the shaking occurs (and before high cellular phone traffic blocks most cell phone use) to a server that can analyze and interpret the data. Further field tests are under way to test the system capabilities.

The cell phones measured seismic parameters such as peak ground acceleration (*PGA*), peak ground velocity (*PGV*), peak ground displacement (*PGD*), and 5% damped spectral accelerations well. In general, iPhone and iPod Touch sensors slightly over-estimated ground motion energy (i.e., Arias Intensity, I_a). However, the mean acceleration response spectrum of the seven iPhones compared remarkably well with that of the reference high quality accelerometers. The error in the recorded intensity parameters was dependent on the characteristics of the input ground motion, particularly its *PGA* and I_a, and decreased for stronger motions. The use of a high-friction device cover (e.g., rubber iPhone covers) on unsecured phones yielded substantially improved data by minimizing independent phone movement. Useful information on the ground motion characteristics was even extracted from unsecured phones during intense shaking events.

The insight gained from these experiments is valuable in distilling information from a large number of imperfect signals from phones that may not be rigidly connected to the ground. With these ubiquitous measurement devices, a more accurate and rapid portrayal of the damage distribution during an earthquake can be provided to emergency responders and to the public.

ACKNOWLEDGEMENTS

Research supported by the U. S. Geological Survey (U.S.G.S.), Department of Interior, under USGS award number G10AP00006. The views and conclusions contained in this document are those of the authors and should not be interpreted as necessarily representing the official policies, either expressed or implied, of the U.S. Government. The financial support of the USGS is gratefully acknowledged. Dr. Rudolph Bonaparte of Geosyntec Consultants inspired the iShake project by suggesting that the accelerometer that is in many smart phones might be used to capture earthquake ground shaking. We would also like to thank Professor Tara Hutchinson at UC San Diego and the staff at the UCSD South Powell Lab for their assistance. They kindly made the small shaking table available for our testing at no charge. We would also like to thank Professor Stephen Mahin at UC Berkeley and PEER, who generously allowed us to mount the phones on the large, multidirectional shaking table at the Richmond Field Station (RFS) during three weeks of an ongoing testing program. Through these experiments, the phone response was studied under realistic earthquake motions at various intensities, which was an essential part of this research project.

TABLE OF CONTENTS

APPENDICES A, B, C, D, E, & F

The appendices are not provided in this electronic version of the technical report to comply with the requirement that the final report be less than 10MB in size.

LIST OF FIGURES

LIST OF TABLES

1 INTRODUCTION

Emergency responders must "see" the effects of an earthquake clearly and rapidly so that they can respond effectively to the damage it has produced. While the USGS has made great strides in developing methodologies that deliver rapid and accurate post-earthquake information, shortcomings exist due to the limited number of strong motion stations available to construct ShakeMaps or due to the qualitative nature of the observations passively obtained from untrained individuals needed to construct "Did You Feel It?" (DYFI)-based maps. The iShake project proposes an innovative use of cell phones and information technology to bridge the gap between the high quality, but sparse, ground motion data that is used to help develop ShakeMap, and the low quality, but large quantity, observational data collected through DYFI.

The DYFI project uses human observations that are voluntarily submitted through the Internet, some time after an earthquake, to develop a Community Internet Intensity Map based largely on the Modified Mercalli Intensity (MMI) scale (Wald et al. 1999). The observations of untrained humans are a rough qualitative indicator of the effects of the earthquake. The speed that this information can be collected and disseminated is dependent on how fast people respond, which might decrease significantly as the level of damage increases in an area.

Rather than using people as measurement "devices," this project proposes using their cell phone to measure ground motion intensity parameters and automatically deliver these data to the USGS for processing and delivery to emergency responders. This research involves the development of the iPhone as a new ad-hoc sensor array based on participatory sensing. The nodes in the sensor array are cell phones voluntarily provided by participants. The objectives of the first phase of the project were the testing and deployment of this new technology.

Dramatic changes in the features commonly available in cellular phones have produced a new breed of phones called smartphones that represent the convergence of sensing, computational power, and communications. Today's smartphones are equipped with a variety of sensors, which include accelerometers, GPS, and cameras. With the emergence of grid computing, numerous operating systems have emerged as these phones become widespread.

A series of 1-D and 3-D shaking table tests were performed as a part of this study, which demonstrated that iPhones (and soon other cellular phones and personal computers that contain accelerometers) can measure reliably the shaking produced by an earthquake. Ground motion parameters such as *PGA*, *PGV*, spectral acceleration, and Arias Intensity are captured accurately by iPhones. Pilot software has been developed that has captured the measured data during the shaking table tests. The data will be sent automatically as a text message immediately after the shaking occurs (and before high cellular phone traffic blocks most cell phone use) to a server that can analyze and interpret the data. Further field tests are under way to test the system capabilities. Additional work is required to make the phone and server software more robust.

The iShake project creates a more objective, quantitative, rapid, and accurate assessment of the distribution of ground shaking produced by a major earthquake. In its eventual field application, relatively high quality shaking data from thousands of cellular phones, whose users have joined the iShake project, will enable the USGS to produce ground shaking maps more rapidly and accurately than can be generated with DYFI. The goal is to create a system that complements DYFI by taking advantage of the accelerometers most people have already in their cell phones, so that an accurate portrayal of the damage effects of an earthquake can be provided to government officials and emergency responders immediately after an event.

2 SENSOR QUALITY EVALUATION

The phone sensor is an imperfect device with variations among a given phone and between phones. The sensor is the entire phone, not just the micro-machined transducer inside. Therefore, the handset needs to be fully calibrated. This characterization requires experiments to answer the following fundamental questions:

- What is the structural effect of the entire phone on the transducer's response?
- How great are the differences between handsets among a manufacturer and between manufacturers?
- What is the severity of the changes in a handset's response over time due to things such as dropping the phone and phone cases, etc.?
- The orientation of the individual sensors will not be known well. What techniques can be used to distill out needed information from the large number of imperfect signals recorded by the mobile phone network?
- How important is the physical mounting of a phone on recorded data?
- What support tools are needed by engineers, public safety agencies, and other stakeholders such as insurance companies? Can we add value to the measurements by being able to extract some pertinent information from a cell phone in a building and one on the ground nearby?

This document summarizes the key preliminary results obtained from the initial shaking table tests and manual experiments performed as a part of this study.

2.1 Shaking Table Tests

2.1.1 Testing Objectives

Four iPhones and three iPod touches were used during shaking table tests to measure acceleration response consistency across multiple sensors and for one phone through multiple identical shakings. The uniaxial shake table at UC San Diego shown in Fig. 1a was used to simulate one-dimensional ground motions of a variety of earthquakes. Subsequently, through the generous contribution of Professor Stephen Mahin of UC Berkeley and PEER, the phone sensors were mounted on the large, multidirectional shaking table at the Richmond Field Station (RFS) during three weeks of shaking (Fig. 1b). This shaking table is configured to produce six degrees of freedom of motion. The shaking table can apply horizontal accelerations of up to 1.5 g to structures weighing up to 100,000 lbs. Through these experiments, the phone response was studied under more realistic, multidirectional earthquake motions at various intensities.

The main objective of these experiments was to better characterize the response of the iPhone and iPod touch as seismic sensors, while simultaneously gaining insight into the seismic response of a free, and potentially falling, instrument. The goal was also to investigate what techniques can be used to distill needed information from a number of imperfect signals recorded by the mobile phones placed at various 3D angles.

(a)

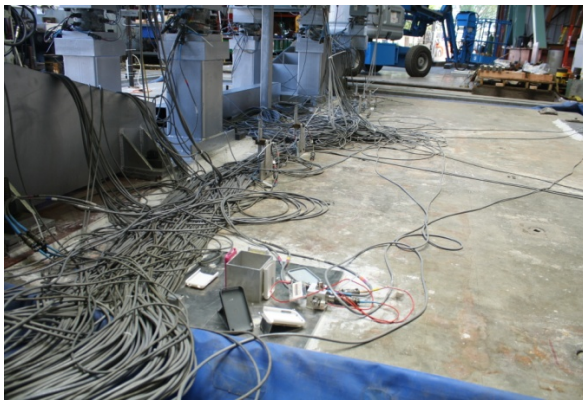

(b)

FIG. 1. Shaking table testing at: (a) UC San Diego South Powell Lab; and (b) UC Berkeley Richmond Field Station facility

2.1.2 iPhone Capabilities and iShake Software Development for Testing

Time synchronization between a set of iPhones was determined to have a guaranteed accuracy of no more than 0.5 seconds. This is due to the drift of the phone's crystal oscillator over time. Although iPhones are regularly updated from cell towers to obtain accurate time, the updates only occur a few times a day; this allows for the drift error to grow. Drift errors may be determined up to millisecond accuracy by using Network Time Protocol (NTP). Client-server communication through NTP allows the server to estimate the client clock drift, and account for the error in later calculations (Lawrence et al. 2008).

An algorithm is required to determine the iPhone's position and orientation from the client. Through the use of the phone's geographical locator, the accelerometers, and the magnetometer, these values were estimated. Gravity and the Earth's magnetic field provide two reference vectors with which the phone can determine its yaw, pitch, and roll. As the Earth's magnetic field is also a function of its position on the earth's surface, it is necessary to know the phone's location. By using the Triad algorithm (Black 1964), the phone's absolute location and orientation may be obtained to the degree of accuracy of the accelerometer and magnetometer. The accelerometer readings must be stationary for a period of time to get a reading of gravity. Hence, an accurate orientation cannot be obtained if the phone is in constant motion.

Because an assessment of steadiness is necessary before measuring a ground motion, a metric was established to classify an iPhone as stable (ready to measure) or unstable (not ready). The metric at this point has two factors: (1) a running sum of the change in the acceleration values, with a memory of 3 to 5 seconds, indicating whether the phone has or has not experienced a substantial amount of shaking within the immediate past; and (2) a maximum absolute difference in acceleration, because the average gravitational readings are taken during the stable period (3 to 5 seconds).

With these metrics implemented, the phone is checked if it has undergone significant movement prior to a ground motion recording. A bonus of this feature is the removal of the possibility of sending false shaking events when a user initially is handling the application. As the iShake system involves the creation of a large client/server system, the software handles this interaction.

For the purposes of recording acceleration data from iPhones on a shake table, an independent pilot application was developed. This client application is able to send and receive commands to and from a server, with a matching application for the server-end of the system. Figure 2 presents the screen shots of the system and phone applications. As shown in the three snapshots, in the prototype version, before the client application can begin to record for earthquake data, the phone must undergo a time frame of stillness. To give a visual representation of the metric to determine a phone's stillness, a "shaking meter" is displayed (Fig. 2a). The development version of the client also includes the possibility of visualizing the shaking on the phone (acceleration, middle screen snapshot) and on the server (Fig. 2a). When operating, the iShake client displays an icon confirming the connectivity of the system (Fig. 2b). As the amount of shaking increases, the meter rises (keeping a certain period of "memory"), and begins recording only when the meter drops below the "safe line."

The system was able to successfully deliver acceleration readings from the phone to the database on the server, at which point the data received could be plotted for instant verification. The implementation of this application serves as a proof of concept for the larger system that must be created for the iShake project.

(a) (b)

FIG. 2. Pilot iShakeTable software: (a) screen shot of server application, and (b) iPhone application

2.1.3 Testing Configuration

Figure 3 shows the testing configuration implemented in these experiments. Three high-quality seismic accelerometers were mounted next to each phone sensor and on the base platform to provide reference accelerations in orthogonal directions. In each test, seven iPhones were mounted on small holders at different 3-D angles. The holders were welded to an 18-inch by 18-inch aluminum platform rigidly bolted to the table. One phone with no cover was free to move about on the table during several shakes at UC San Diego (ST-1). Subsequently, two phones with different types of covers were left free to move on the table and fall during several 3-D shakes at the Richmond Field Station (ST-2).

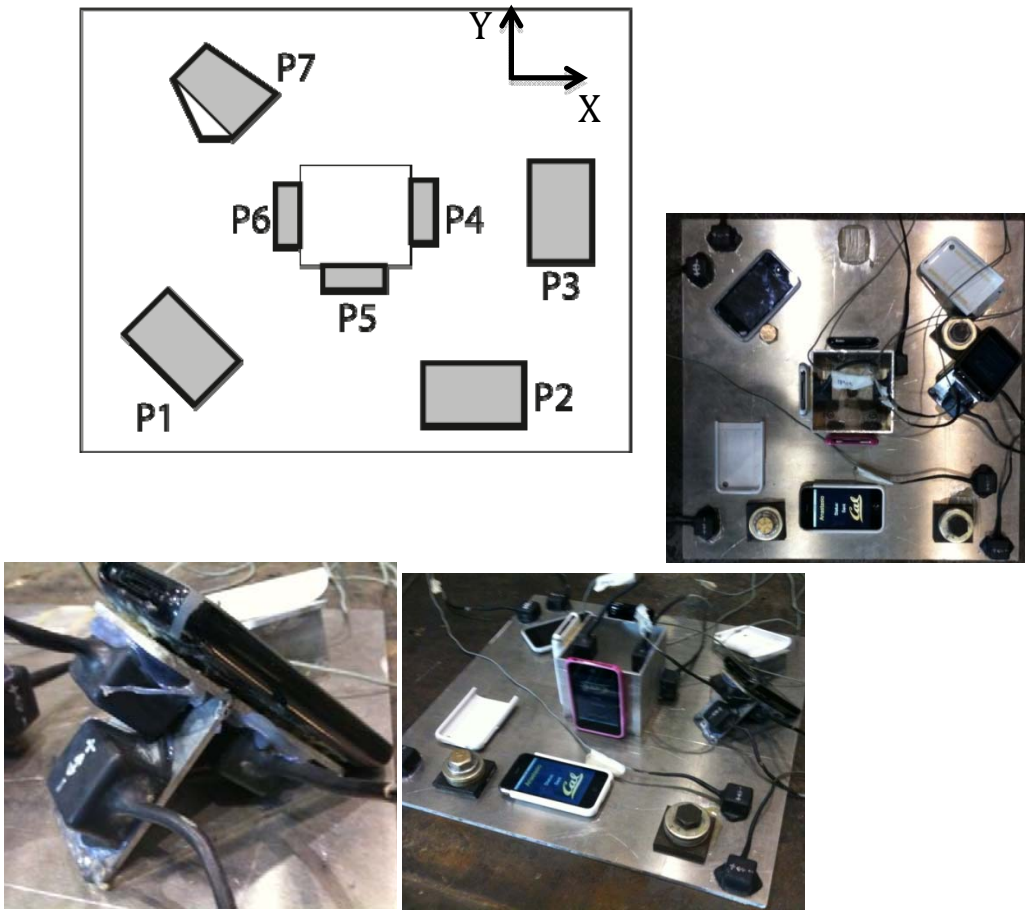

FIG 3. Phone and instrumentation set up during the shaking table tests (shaking applied in the x-direction during ST-1)

Table 1 summarizes the sequence of ground motions applied in the first shaking table test at UC San Diego (ST-1). A suite of 38 one-dimensional (1-D) realistic ground motions at various intensity levels in addition to a synthetic record and 15 sine sweeps were applied to the base platform during a total of 86 shaking events. A smaller group of selected 1-D ground motions were subsequently repeated at different intensity levels. These earthquake ground motions were primarily selected based on probabilistic seismic hazard analyses for a site in downtown Los Angeles (Mason et al. 2010) and for the University of California, Berkeley campus (Wong et al. 2008). Fig. 4 presents the acceleration response spectra (5% damped) and Arias Intensity-time

histories of the input motions at their original scale. These ground motions were chosen primarily because the methodologies are being developed and tested in California first. The seismic hazard at these two sites was mostly dominated by near fault events with the forward directivity effect. The chosen motions were mainly recorded at sites classified as C or D. Moreover, a number of less intense, strike slip events recorded at a large distance from faults were chosen to better study the mobile sensor's response for a wide range of ground motions. The original recorded in situ ground motions were modified to reduce displacements to the allowed stroke of the shaking table at UC San Diego (+/- 150 mm). Table 2 provides the complete list of the recorded or achieved ground motions in ST-1. The *SIR* parameter in these tables refers to the Shaking Intensity Rate defined by Dashti et al. (2010) as the slope of the Arias Intensity-time history:

$$SIR = I_{a5\text{-}75}/D_{5\text{-}75} \quad (2)$$

where $I_{a5\text{-}75}$ is the change in Arias Intensity from 5% to 75% of its total value, and $D_{5\text{-}75}$ is its corresponding time duration. This is a useful parameter in Geotechnical Earthquake Engineering Applications.

Table 3 presents the list of 3-D input ground motions selected during the shaking table tests performed at UC Berkeley's Richmond Field Station (ST-2). Five primary earthquake ground motions were applied at various directions and intensities in addition to a number of sine-sweeps, adding to forty 3-D input ground motion combinations. Tables 4 through 6 provide a complete list of the recorded or achieved ground motions in ST-2 in the x, y, and z directions, respectively.

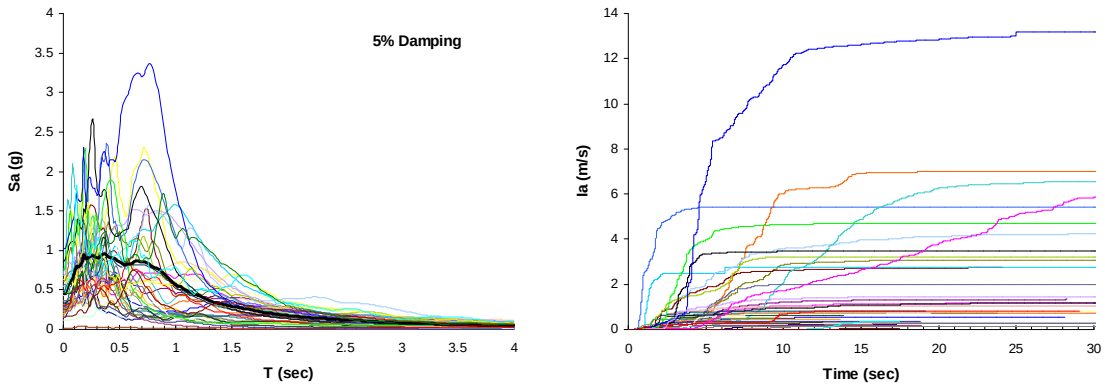

FIG. 4. Acceleration Response Spectra (5% damped) and Arias Intensity-time histories of the 1-D input ground motions in ST-1

Table 1. List of 1-D input earthquake ground motions selected in ST-1

Earthquake	M_w	Station	R_{close} (km)	Site	Scale	PGA (g)	PGV (cm/s)	PGD (cm)	D_{5-95} (sec)	T_m (sec)	I_a (m/sec)
79 Imperial Valley	6.5	Brawley Airport 225	8.5	C	1.00	0.16	25.3	13.1	15.2	0.93	0.28
89 Loma Prieta	7	Saratoga W V Coll 270	13.7	C	1.00	0.36	49.33	14.36	10.58	0.92	1.17
		LGPC 090	6.1	C	1.00	0.6	50.92	11.5	7.82	0.55	3.09
		Los Gatos Presentation Center 218	3.5	C	1.00	0.63	62.96	15.73	7.48	0.61	7
		Saratoga Aloha Ave 218	8.3	C	1.00	0.33	45.1	15.5	8.5	0.65	1.3
		Corralitos 218	3.4	C	1.00	0.47	44.57	13.82	7.8	0.58	2.73
		Gavilan College 218	9.5	C	1.00	0.29	30.2	6.39	5.16	0.35	0.74
		Gilroy historic 218	-	C	1.00	0.28	31.32	8.4	11.36	0.7	0.56
		Lexington Dam Abutment 218	6.3	C	1.00	0.5	74.8	15.8	4.22	0.93	2.5
		Hayward Bart Station 310	54.15	C,D	1.00	0.16	102.6	3.32	13.2	0.36	0.28
		Berkeley LBL 090	79.25	C	1.00	0.12	20.9	4.43	7.98	0.89	0.15
		Treasure Island 090	82.9	D	1.00	0.16	32.7	11.5	4.4	1.1	0.36
99 Kocaeli	7.4	Ambarli090	78.9	D	2.00	0.46	60.57	12.24	34.4	0.9	4.62
94 Northridge	6.7	Newhall - W Pico Cany 046	7.1	C	0.73	0.233	48	13.5	7.1	1.26	0.61
		Sylmar - Conv Sta 052	6.2	C	0.92	0.54	86.2	15.5	15.3	0.9	4.3
		Rinaldi R Sta 228	7.1	C	0.73	0.69	75.9	15	6.84	0.65	3.6

Table 1. List of 1-D input earthquake ground motions selected in ST-1 (continued)

Earthquake	M_w	Station	$R_{closest}$ (km)	Site Classif.	Scale	PGA (g)	PGV (cm/s)	PGD (cm)	D_{5-95} (sec)	T_m (sec)	I_a (m/sec)
95 Kobe	6.9	Port Island (0m) 090	2.5	D	1.00	0.24	46.4	14.7	11.58	1.18	1
		Kobe JMA 090	0.5	C	1.00	0.56	76.8	14.3	9.5	0.65	5.43
92 Landers	7.3	Lucerne 260	1.1	C	1.00	0.695	48.5	14.38	13.6	0.22	6.6
		Joshua Tree 090	11.3	C	1.17	0.32	41.67	15.4	26.08	0.77	3.21
99 Chi Chi	7.6	TCU078 270 (E)	8.2	C	0.45	0.2	17.67	14.07	25.92	0.43	1.17
71 San Fernando	6.6	LA Hollywood Stor Lot 180	22.77	D	1.00	0.17	14.84	6.29	11.16	0.35	0.45
87 Supertition Hills	6.6	Parachute T S 315	0.95	D	0.66	0.25	28.96	10.12	11.07	0.67	0.74
		Superstition Mnt Cam 045	5.61	C	0.73	0.5	23.73	3.43	12.28	0.33	1.97
79 Coyote Lake	5.7	Coyote Lake Dam Abutment 066	4	C	1.00	0.27	19.4	2.19	5.21	0.46	0.34
		Gilroy #6 066	1.2	C	1.00	0.44	50.56	6.96	3.4	0.61	0.82
66 Parkfield	6	Temblor 047	4.4	C	1.00	0.36	21.99	4.5	3.96	0.4	0.5
		Array #5 047	3.7	D	1.00	0.32	22.49	4.65	7.06	0.44	0.63
		Array #8 047	8	D	1.00	0.24	10.25	3.41	13.17	0.39	0.29
80 Livermore	5.5	Fagundes Ranch 053	4.1	D	1.00	0.22	13.32	0.8	2.83	0.34	0.17
		Morgan Territory Park 053	8.1	C	1.00	0.29	14.63	1.07	2.82	0.24	0.36
84 Morgan Hill	6.2	Coyote Lake Dam Abutment 244	0.1	C	1.00	0.85	65.91	9.68	2.71	0.48	3.48
		Anderson Dam Downstream 244	4.5	C	1.00	0.43	26.74	4.19	6.51	0.42	0.7
		Halls Valley 244	2.5	C	1.00	0.3	38.13	7.4	10.64	0.6	0.82
2000 Tottori, Japan	6.6	Kofu 238	10	C	1.00	0.76	36.4	7.86	8	0.27	4.67
		Hino 238	1	C	1.00	1.02	98.69	14.85	7.99	0.59	13
92 Erzincan, Turkey	6.7	Erzincan 030	1.8	C	1.00	0.44	48.8	14.98	8.9	0.68	1.46

Table 2. Complete list of recorded (achieved) ground motions during ST-1

Trial	Name	PGA [g's]	PGV [cm/s]	PGD [cm]	Sa(T=1s) [g]	Sa(T=3s) [g]	D5-95 [sec]	Arias Intensity [m/s]	SIR [m/s^2]
1	1979 Imperial Valley -- Brawley Airport 225	0.18	17.24	4.88	0.17	0.30	16.83	0.29	0.03
2	1979 Imperial Valley -- 6605 Delta 352	0.62	40.96	10.39	0.49	1.14	45.86	8.09	0.26
3	1989 Loma Prieta -- Saratoga Aloha Ave. 218	0.37	33.69	7.59	0.51	0.90	9.05	1.49	0.25
5	1989 Loma Prieta -- LGPC 090	0.45	33.78	7.48	0.43	1.17	8.46	3.53	0.44
6	1989 Loma Prieta -- Saratoga W V Coll. 270	0.33	39.21	8.29	0.64	0.75	12.32	1.24	0.19
7	1989 Loma Prieta -- Los Gatos Presentation Center 218 (50% Intensity)	0.49	28.30	3.83	0.43	0.69	10.34	2.05	0.27
8	1989 Loma Prieta -- Corralitos 218	0.55	41.21	5.55	0.47	1.32	8.56	3.15	0.50
9	1989 Loma Prieta -- Gavilan College 218	0.35	15.25	3.83	0.22	0.83	5.78	0.89	0.38
10	1989 Loma Prieta -- Gilroy Historic 218	0.21	17.33	4.70	0.24	0.60	13.03	0.66	0.10
12	1989 Loma Prieta -- Hayward Bart Station 310	0.19	9.08	1.11	0.12	0.23	15.07	0.39	0.04
13	1989 Loma Prieta -- Lexington Dam Abutment 218 (50% Intensity)	0.31	29.84	5.14	0.70	0.33	4.32	0.66	0.22
14	1989 Loma Prieta -- Berkeley LBL 090	0.19	16.81	2.64	0.28	0.24	16.08	0.19	0.05
15	1999 Kocaeli -- Abmarli 090 (50% Intensity)	0.21	30.06	5.40	0.59	0.58	37.37	1.36	0.11
16	1994 Northridge -- Newhall - W Pico Cany. 046 (80% Intensity)	0.20	27.30	8.15	0.50	0.31	11.35	0.39	0.08
17	1994 Northridge -- Sylmar Conv. Station 052 (50% Intensity)	0.31	35.70	3.70	0.60	0.50	16.47	1.10	0.15
18	1994 Northridge -- Rinaldi R Station 228 (50% Intensity)	0.29	27.63	4.90	0.49	0.68	7.18	0.98	0.18
19	1995 Kobe -- Port Island (0m) 090	0.34	32.56	7.20	0.82	0.40	11.47	1.00	0.18
20	1995 Kobe -- JMA 090 (50% Intensity)	0.33	31.01	3.95	0.43	1.16	10.92	1.60	0.25
21	1992 Landers -- Lucerne 260	0.69	33.47	6.27	0.49	0.75	12.46	6.12	0.54
22	1992 Landers -- Joshua Tree 090	0.27	30.64	5.25	0.71	0.93	26.29	3.53	0.11

Table 2. Complete list of recorded (achieved) ground motions during ST-1 (continued)

Trial	Name	PGA [g's]	PGV [cm/s]	PGD [cm]	Sa(T=1s) [g]	Sa(T=3s) [g]	D5-95 [sec]	Arias Intensity [m/s]	SIR [m/s^2]
23	1999 Chi-Chi Taiwan -- TCU078 270 E	0.26	13.13	2.44	0.16	0.73	26.85	1.49	0.07
24	1971 San Fernando -- LA Hollywood Stor Lot 180	0.22	8.58	2.16	0.12	0.32	12.65	0.53	0.07
25	1987 Superstition Hills -- Parachute T S 315	0.19	18.88	3.45	0.35	0.61	11.43	0.89	0.08
26	1987 Superstition Hills -- Superstition Mnt Cam 045	0.50	19.67	3.01	0.21	0.71	12.14	2.35	0.18
27	1979 Coyote Lake -- Coyote Lake Dam Abutment 066	0.29	12.55	1.65	0.11	0.70	7.83	0.42	0.19
28	1979 Coyote Lake -- Gilroy #6 066	0.22	38.00	7.83	0.46	0.87	5.91	0.93	0.51
29	1966 Parkfield -- Temblor 047	0.47	17.78	1.94	0.19	1.06	5.26	0.62	0.31
30	1966 Parkfield -- Array #5 047	0.38	13.39	2.02	0.14	1.09	7.62	0.79	0.22
31	1966 Parkfield -- Array #8 047	0.19	8.03	1.27	0.11	0.31	15.24	0.36	0.04
32	1980 Livermore -- Fagundes Ranch 053	0.19	13.86	0.84	0.04	0.69	3.63	0.22	0.23
33	1980 Livermore -- Morgan Territory Park 053	0.30	11.86	0.80	0.10	0.29	3.43	0.42	0.34
34	1984 Morgan Hill -- Coyote Lake Dam Abutment 244 (70% Intensity)	0.77	33.95	3.06	0.42	1.26	2.47	1.95	1.04
35	1984 Morgan Hill -- Anderson Dam Downstream 244	0.37	17.56	1.92	0.13	1.01	7.38	0.88	0.28
36	1984 Morgan Hill -- Halld Valley 244	0.27	34.06	5.75	0.39	0.58	11.28	1.00	0.08
37	2000 Tottori - Japan -- Kofu 238	0.56	25.81	3.03	0.13	1.28	8.17	5.22	1.01
38	2000 Tottori - Japan -- Hino 238 (50% Intensity)	0.46	49.57	5.73	0.55	1.11	9.60	3.81	0.64
39	1992 Erzincan - Turkey -- Erzincan 030	0.58	30.21	5.54	0.48	1.05	9.56	1.59	0.30
40	1989 Loma Prieta -- Treasure Island 090	0.21	27.24	6.64	0.21	0.51	4.79	0.38	0.08
41	1989 Loma Prieta -- Gilroy Historic 218	0.23	17.35	4.58	0.24	0.60	12.55	0.65	0.10
42	1966 Parkfield -- Temblor 047	0.46	17.86	1.90	0.19	1.06	5.04	0.62	0.31
43	UCSD Synthetic (10% Intensity)	0.32	10.29	0.90	0.06	0.70	24.45	3.25	0.12

Table 2. Complete list of recorded (achieved) ground motions during ST-1 (continued)

Trial	Name	PGA [g's]	PGV [cm/s]	PGD [cm]	Sa(T=1s) [g]	Sa(T=3s) [g]	D5-95 [sec]	Arias Intensity [m/s]	SIR [m/s^2]
44	UCSD Synthetic (50% Intensity)	1.83	48.26	4.46	0.27	3.44	25.17	85.70	3.05
45	1992 Landers -- Joshua Tree 090 (34% Intensity)	0.14	10.62	1.82	0.24	0.31	26.87	0.47	0.01
46	1992 Landers -- Joshua Tree 090 (34% Intensity)	0.14	10.63	1.82	0.24	0.29	26.51	0.47	0.01
47	1992 Landers -- Joshua Tree 090 (57% Intensity)	0.19	17.36	3.06	0.40	0.50	26.42	1.20	0.04
48	1992 Landers -- Joshua Tree 090 (57% Intensity)	0.19	17.41	3.05	0.40	0.51	26.43	1.20	0.04
49	1992 Landers -- Joshua Tree 090 (100% Intensity)	0.27	30.61	5.34	0.70	0.92	26.27	3.47	0.11
50	1995 Kobe -- JMA 090 (8% Intensity)	0.09	5.05	0.66	0.07	0.17	13.02	0.06	0.01
51	1995 Kobe -- JMA 090 (24% Intensity)	0.18	14.94	1.87	0.21	0.54	11.34	0.40	0.06
52	1995 Kobe -- JMA 090 (24% Intensity)	0.18	15.08	1.88	0.21	0.54	11.23	0.40	0.06
53	1995 Kobe -- JMA 090 (41% Intensity)	0.28	25.50	3.35	0.35	0.94	10.92	1.08	0.17
54	1995 Kobe -- JMA 090 (50% Intensity)	0.33	30.85	3.89	0.43	1.16	10.90	1.58	0.25
55	1994 Northridge -- Sylmar Conv. Station 052 (11% Intensity)	0.12	8.09	0.77	0.13	0.12	24.34	0.08	0.01
56	1994 Northridge -- Sylmar Conv. Station 052 (33% Intensity)	0.23	23.57	2.40	0.40	0.34	17.71	0.50	0.07
57	1994 Northridge -- Sylmar Conv. Station 052 (33% Intensity)	0.23	23.51	2.43	0.40	0.34	17.68	0.50	0.07
58	1994 Northridge -- Sylmar Conv. Station 052 (55% Intensity)	0.34	39.42	4.04	0.66	0.56	16.08	1.31	0.18
59	1994 Northridge -- Sylmar Conv. Station 052 (55% Intensity)	0.32	39.30	4.04	0.66	0.56	16.28	1.30	0.18
60	1999 Chi-Chi Taiwan -- TCU078 270 E (57% Intensity)	0.17	7.40	1.37	0.09	0.41	27.69	0.53	0.02

Table 2. Complete list of recorded (achieved) ground motions during ST-1 (continued)

Trial	Name	PGA [g's]	PGV [cm/s]	PGD [cm]	Sa(T=1s) [g]	Sa(T=3s) [g]	D5-95 [sec]	Arias Intensity [m/s]	SIR [m/s^2]
61	1999 Chi-Chi Taiwan -- TCU078 270 E (57% Intensity)	0.17	7.88	1.36	0.09	0.40	27.61	0.54	0.02
62	1999 Chi-Chi Taiwan -- TCU078 270 E (100% Intensity)	0.24	13.61	2.43	0.17	0.72	26.78	1.46	0.06
63	1999 Chi-Chi Taiwan -- TCU078 270 E (190% Intensity)	0.42	24.78	4.48	0.31	1.42	26.38	4.95	0.22
64	1999 Chi-Chi Taiwan -- TCU078 270 E (190% Intensity)	0.42	25.17	4.50	0.31	1.40	26.38	4.95	0.22
65	1989 Loma Prieta -- Saratoga W V Coll. 270 (16% Intensity)	0.08	6.38	1.34	0.10	0.12	22.65	0.05	0.01
66	1989 Loma Prieta -- Saratoga W V Coll. 270 (48% Intensity)	0.21	19.32	3.97	0.30	0.38	14.32	0.32	0.05
67	1989 Loma Prieta -- Saratoga W V Coll. 270 (48% Intensity)	0.21	19.38	4.02	0.30	0.37	14.24	0.31	0.05
68	1989 Loma Prieta -- Saratoga W V Coll. 270 (81% Intensity)	0.28	31.89	6.80	0.52	0.61	12.73	0.83	0.14
69	1989 Loma Prieta -- Saratoga W V Coll. 270 (100% Intensity)	0.33	39.39	8.36	0.64	0.75	11.56	1.22	0.21
70	Sine-Wave 1: Amp = 0.1g - Freq = 0.5Hz	0.15	26.75	8.69	0.14	0.11	34.79	2.26	0.06
71	Sine-Wave 2: Amp = 0.1g - Freq = 1Hz	0.19	16.09	2.59	0.51	0.13	25.52	2.41	0.08
72	Sine-Wave 3: Amp = 0.1g - Freq = 2Hz	0.19	8.86	0.75	0.03	0.21	24.75	2.85	0.10
73	Sine-Wave 4: Amp = 0.1g - Freq = 4Hz	0.17	5.14	0.32	0.01	0.15	25.69	3.19	0.11
74	Sine-Wave 5: Amp = 0.3g - Freq = 1Hz	0.37	47.32	7.66	1.55	0.45	26.68	21.11	0.71
75	Sine-Wave 6: Amp = 0.3g - Freq = 2Hz	0.39	25.31	2.14	0.10	0.62	27.43	25.08	0.83

Table 2. Complete list of recorded (achieved) ground motions during ST-1 (continued)

Trial	Name	PGA [g's]	PGV [cm/s]	PGD [cm]	Sa(T=1s) [g]	Sa(T=3s) [g]	D5-95 [sec]	Arias Intensity [m/s]	SIR [m/s^2]
76	Sine-Wave 7: Amp = 0.3g - Freq = 4Hz	0.35	12.95	0.59	0.02	0.43	27.55	24.70	0.81
77	Sine-Wave 8: Amp = 0.3g - Freq = 1Hz	0.37	47.29	7.68	1.54	0.45	27.96	22.07	0.71
78	Sine-Wave 9: Amp = 0.3g - Freq = 2Hz	0.40	25.30	2.11	0.09	0.61	27.43	25.12	0.83
79	Sine-Wave 10: Amp = 0.3g - Freq = 4Hz	0.36	13.10	0.63	0.03	0.42	27.85	25.00	0.81
80	Sine-Wave 11: Amp = 0.5g - Freq = 2Hz	0.64	41.70	3.53	0.15	1.00	27.21	68.28	2.26
81	Sine-Wave 12: Amp = 0.5g - Freq = 4Hz	0.59	21.51	1.00	0.04	0.74	26.70	67.68	2.28

Table 3. List of 3-D input ground motions selected in ST-2

Ground Motion	Motion ID	Direction
1978 Tabas, Iran	nf01.AT2	UX
	nf02.AT2	UY
	nf0102v.AT2	UZ
1995 KJMA, Kobe	KJM000.AT2	UX or UY
	KJM090.AT2	UY or UX
	KJMUP.AT2	UZ
1994 Sylmar, Northridge PEER	SYL360.AT2	UX or UY
	SYL090.AT2	UY or UX
	SYLvertical.AT2	UZ
2010 Chile	CHILE_2010_X.AT2	UY
	CHILE_2010_Y.AT2	UX
	CHILE_2010_Z.AT2	UZ
1985 Llolleo, Chile	SE17.AT2	UX
	SE18.AT2	UY
Description of Ground Motions		
1978 Tabas, Iran (SAC System Performance Ground Motions)		
1995 Kobe, Japan (KJMA Station, PEER Strong Motion Database)		
1994 Northridge, California (Sylmar - Olive View Med FF Station, PEER Strong Motion Database)		
2010 Chile (Classified)		
1985 Llolleo, Chile (SAC System Performance Ground Motions)		

Table 4. Complete list of recorded (achieved) ground motions in x-direction during ST-2

Motion No.	Name	PGA [g's]	PGV [cm/s]	PGD [cm]	Sa(T=1s) [g]	Sa(T=3s) [g]	D5-95 [sec]	Arias Intensity [m/s]	SIR [m/s^2]
14	Sin Sweep X	0.07	3.95	1.23	0.06	0.21	35.35	0.13	0.00
15	Sin Sweep X	0.16	7.47	2.46	0.12	0.47	28.05	0.31	0.03
17	SinX T 188 6cycle	0.06	7.28	2.01	0.08	0.06	9.67	0.08	0.01
18	SinX T 188 6cycle	0.12	13.99	4.00	0.15	0.11	9.58	0.23	0.02
20	1995 KJMA - Kobe UXUYUZ 100	0.15	5.19	0.45	0.03	0.23	4.53	0.11	0.04
21	1995 KJMA - Kobe UXUYUZ 100	0.20	11.92	0.83	0.05	0.47	4.41	0.35	0.12
27	1995 KJMA - Kobe UXUYUZ 100	0.19	11.19	0.86	0.05	0.45	6.51	0.35	0.11
33	1995 KJMA - Kobe UXUYUZ 100	0.38	23.15	1.63	0.10	0.96	4.64	1.25	0.43
38	1995 KJMA - Kobe UXUYUZ 100	0.25	15.49	1.07	0.07	0.66	4.96	0.63	0.21
39	1995 KJMA - Kobe UXUYUZ 100	0.26	15.73	1.04	0.06	0.66	5.01	0.66	0.22
40	1995 KJMA - Kobe UXUYUZ 100	0.38	23.50	1.50	0.10	0.95	4.88	1.22	0.41
41	1995 KJMA - Kobe UXUYUZ 100	0.37	22.53	1.62	0.09	0.94	4.65	1.28	0.43
42	1978 Tabas - Iran UXUYUZ 100	0.13	9.73	2.30	0.10	0.22	18.95	0.26	0.03
43	1978 Tabas - Iran UXUYUZ 100	0.15	11.55	2.79	0.12	0.26	13.21	0.30	0.04
44	1978 Tabas - Iran UXUYUZ 100	0.15	11.90	2.83	0.12	0.26	13.05	0.32	0.04
45	1978 Tabas - Iran UXUYUZ 100	0.38	22.58	5.60	0.24	0.52	12.24	1.19	0.16
61	1994 Sylmar - Northridge PEER XYZ ROT 60 CW	0.49	18.30	2.65	0.29	0.91	2.94	1.19	0.54
62	1995 KJMA - Kobe UYUXUZ 100	0.32	18.51	1.39	0.08	0.73	5.13	0.81	0.25
63	1995 KJMA - Kobe UYUXUZ 100	0.44	21.67	1.65	0.10	0.87	4.28	1.12	0.36
64	1995 KJMA - Kobe UYUXUZ 100	0.44	25.28	1.81	0.12	0.97	4.14	1.46	0.47
65	1995 KJMA - Kobe UYUXUZ 100	0.60	30.22	2.05	0.13	1.11	4.34	1.95	0.62

Table 4. Complete list of recorded (achieved) ground motions in x-direction during ST-2 (continued)

Motion No.	Name	PGA [g's]	PGV [cm/s]	PGD [cm]	Sa(T=1s) [g]	Sa(T=3s) [g]	D5-95 [sec]	Arias Intensity [m/s]	SIR [m/s^2]
66	1994 Sylmar - Northridge PEER rot 300 CW	0.36	14.92	2.30	0.24	0.58	2.68	0.49	0.22
67	1994 Sylmar - Northridge PEER rot 300 CW	0.55	20.16	3.12	0.32	0.76	2.59	0.85	0.39
142	1978 Tabas - Iran UXUYUZ 100	0.11	8.89	2.20	0.10	0.21	13.64	0.18	0.02
143	1978 Tabas - Iran UXUYUZ 100	0.25	17.97	4.42	0.19	0.43	12.57	0.69	0.10
144	1994 Sylmar - Northridge PEER UXUYUZ 100	0.26	13.48	2.32	0.33	0.24	4.13	0.33	0.12
145	1994 Sylmar - Northridge PEER UXUYUZ 100	0.10	5.11	0.90	0.12	0.12	9.23	0.06	0.02
146	1994 Sylmar - Northridge PEER UXUYUZ 100	0.15	8.24	1.45	0.20	0.17	2.86	0.13	0.05
147	1978 Tabas - Iran UXUYUZ 100	0.39	31.09	7.73	0.33	0.75	11.38	1.98	0.29
148	1994 Sylmar - Northridge PEER UXUYUZ 100	0.41	19.23	3.44	0.49	0.50	3.72	0.67	0.23
149	1995 KJMA - Kobe UYUXUZ 100	0.60	32.61	2.21	0.14	1.15	3.99	2.07	0.68
150	SinY T 200 6cycle	0.12	19.05	5.74	0.19	0.14	10.18	0.36	0.03
151	1995 KJMA - Kobe UYUXUZ 100	0.37	21.38	1.59	0.10	0.83	4.64	1.01	0.33
153	1978 Tabas - Iran UXUYUZ 100	0.27	19.38	4.89	0.21	0.47	11.00	0.84	0.12
155	1978 Tabas - Iran UXUYUZ 100	0.21	14.22	3.57	0.15	0.34	13.72	0.48	0.07
156	1994 Sylmar - Northridge PEER UXUYUZ 100	0.26	12.60	2.32	0.33	0.27	4.65	0.33	0.11
162	1978 Tabas - Iran UXUYUZ 100	0.39	30.03	7.48	0.32	0.73	9.94	1.94	0.29
163	1978 Tabas - Iran UXUYUZ 100	0.39	30.20	7.49	0.32	0.74	9.99	2.00	0.30
164	1978 Tabas - Iran UXUYUZ 100	0.40	30.52	7.58	0.32	0.75	10.47	1.98	0.31
165	1978 Tabas - Iran UXUYUZ 100	0.40	30.56	7.52	0.33	0.75	10.30	1.98	0.31
166	1978 Tabas - Iran UXUYUZ 100	0.27	19.25	4.79	0.21	0.46	10.69	0.82	0.13

Table 5. Complete list of recorded (achieved) ground motions in y-direction during ST-2

Motion No.	Name	PGA [g's]	PGV [cm/s]	PGD [cm]	Sa(T=1s) [g]	Sa(T=3s) [g]	D5-95 [sec]	Arias Intensity [m/s]	SIR [m/s^2]
14	Sin Sweep X	0.08	3.97	1.24	0.06	0.21	35.34	0.13	0.00
15	Sin Sweep X	0.16	7.59	2.48	0.12	0.47	30.13	0.33	0.03
17	SinX T 188 6cycle	0.07	7.37	2.03	0.08	0.06	9.72	0.08	0.01
18	SinX T 188 6cycle	0.12	14.06	4.02	0.15	0.11	9.58	0.23	0.02
20	1995 KJMA - Kobe UXUYUZ 100	0.16	7.01	1.03	0.07	0.24	4.17	0.17	0.07
21	1995 KJMA - Kobe UXUYUZ 100	0.25	13.39	1.73	0.12	0.52	3.68	0.42	0.16
27	1995 KJMA - Kobe UXUYUZ 100	0.26	13.76	1.62	0.11	0.56	5.34	0.50	0.17
33	1995 KJMA - Kobe UXUYUZ 100	0.39	24.96	3.05	0.22	1.10	4.15	1.59	0.54
38	1995 KJMA - Kobe UXUYUZ 100	0.34	18.25	2.40	0.17	0.73	4.43	0.77	0.27
39	1995 KJMA - Kobe UXUYUZ 100	0.27	16.90	1.68	0.13	0.80	4.98	0.78	0.25
40	1995 KJMA - Kobe UXUYUZ 100	0.49	25.52	2.65	0.19	1.13	4.16	1.62	0.55
41	1995 KJMA - Kobe UXUYUZ 100	0.36	24.86	2.91	0.22	1.07	4.13	1.61	0.55
42	1978 Tabas - Iran UXUYUZ 100	0.14	6.83	1.45	0.06	0.17	20.20	0.22	0.02
43	1978 Tabas - Iran UXUYUZ 100	0.14	7.34	1.54	0.07	0.18	15.09	0.21	0.02
44	1978 Tabas - Iran UXUYUZ 100	0.15	7.32	1.59	0.07	0.19	14.92	0.23	0.03
45	1978 Tabas - Iran UXUYUZ 100	0.30	15.35	3.06	0.14	0.33	13.34	0.73	0.10
61	1994 Sylmar - Northridge PEER XYZ ROT 60 CW	0.30	11.51	1.66	0.24	0.32	5.97	0.27	0.09
62	1995 KJMA - Kobe UYUXUZ 100	0.40	14.17	1.09	0.08	0.94	6.98	0.71	0.21
63	1995 KJMA - Kobe UYUXUZ 100	0.45	16.53	1.18	0.09	1.13	5.49	0.97	0.30
64	1995 KJMA - Kobe UYUXUZ 100	0.50	22.64	1.95	0.14	1.15	5.07	1.20	0.36
65	1995 KJMA - Kobe UYUXUZ 100	0.69	21.98	1.61	0.12	1.49	4.95	1.74	0.57
66	1994 Sylmar - Northridge PEER rot 300 CW	0.17	10.17	1.03	0.09	0.33	6.68	0.28	0.08

Table 5. Complete list of recorded (achieved) ground motions in y-direction during ST-2 (continued)

Motion No.	Name	PGA [g's]	PGV [cm/s]	PGD [cm]	Sa(T=1s) [g]	Sa(T=3s) [g]	D5-95 [sec]	Arias Intensity [m/s]	SIR [m/s^2]
67	1994 Sylmar - Northridge PEER rot 300 CW	0.27	13.30	1.32	0.12	0.47	5.30	0.48	0.18
142	1978 Tabas - Iran UXUYUZ 100	0.16	6.17	1.43	0.06	0.14	13.07	0.26	0.03
143	1978 Tabas - Iran UXUYUZ 100	0.25	13.82	2.85	0.15	0.34	14.66	0.54	0.07
144	1994 Sylmar - Northridge PEER UXUYUZ 100	0.23	11.01	1.47	0.15	0.40	6.07	0.33	0.11
145	1994 Sylmar - Northridge PEER UXUYUZ 100	0.11	4.10	0.59	0.06	0.18	12.07	0.06	0.02
146	1994 Sylmar - Northridge PEER UXUYUZ 100	0.15	6.29	0.96	0.10	0.26	3.48	0.12	0.04
147	1978 Tabas - Iran UXUYUZ 100	0.33	18.88	4.24	0.18	0.48	10.74	1.18	0.15
148	1994 Sylmar - Northridge PEER UXUYUZ 100	0.45	16.07	2.19	0.23	0.43	4.65	0.65	0.19
149	1995 KJMA - Kobe UYUXUZ 100	0.69	22.09	1.76	0.12	1.52	4.66	1.78	0.62
150	SinY T 200 6cycle	0.04	2.06	0.29	0.04	0.04	10.80	0.01	0.00
151	1995 KJMA - Kobe UYUXUZ 100	0.42	16.60	1.21	0.09	1.06	5.30	0.86	0.28
153	1978 Tabas - Iran UXUYUZ 100	0.24	13.84	2.89	0.13	0.33	12.73	0.53	0.07
155	1978 Tabas - Iran UXUYUZ 100	0.16	10.20	2.14	0.10	0.25	18.00	0.32	0.04
156	1994 Sylmar - Northridge PEER UXUYUZ 100	0.23	10.97	1.44	0.15	0.36	5.53	0.30	0.09
162	1978 Tabas - Iran UXUYUZ 100	0.28	18.56	3.94	0.17	0.46	10.57	1.18	0.16
163	1978 Tabas - Iran UXUYUZ 100	0.30	18.68	3.95	0.18	0.46	10.36	1.22	0.16
164	1978 Tabas - Iran UXUYUZ 100	0.30	18.27	4.12	0.18	0.47	10.54	1.26	0.16
165	1978 Tabas - Iran UXUYUZ 100	0.30	18.42	4.05	0.18	0.46	10.52	1.27	0.16
166	1978 Tabas - Iran UXUYUZ 100	0.27	13.69	2.89	0.14	0.32	11.97	0.57	0.08

Table 6. Complete list of recorded (achieved) ground motions in z-direction during ST-2

Motion No.	Name	PGA [g's]	PGV [cm/s]	PGD [cm]	Sa(T=1s) [g]	Sa(T=3s) [g]	D5-95 [sec]	Arias Intensity [m/s]	SIR [m/s^2]
14	Sin Sweep X	0.02	0.33	0.05	0.00	0.01	34.64	0.03	0.00
15	Sin Sweep X	0.02	0.70	0.21	0.01	0.02	34.58	0.03	0.00
17	SinX T 188 6cycle	0.03	9.12	3.36	0.05	0.05	8.80	0.02	0.00
18	SinX T 188 6cycle	0.02	0.68	0.13	0.01	0.01	10.09	0.01	0.00
20	1995 KJMA - Kobe UXUYUZ 100	0.11	5.61	0.36	0.03	0.31	5.33	0.08	0.03
21	1995 KJMA - Kobe UXUYUZ 100	0.18	9.36	0.69	0.05	0.57	4.75	0.21	0.07
27	1995 KJMA - Kobe UXUYUZ 100	0.19	10.16	0.82	0.06	0.46	5.22	0.18	0.06
33	1995 KJMA - Kobe UXUYUZ 100	0.41	18.59	1.35	0.10	1.13	4.65	0.87	0.28
38	1995 KJMA - Kobe UXUYUZ 100	0.25	12.42	0.84	0.06	0.78	4.72	0.42	0.13
39	1995 KJMA - Kobe UXUYUZ 100	0.23	13.67	1.05	0.08	0.70	4.67	0.36	0.12
40	1995 KJMA - Kobe UXUYUZ 100	0.37	19.82	1.45	0.12	1.02	4.66	0.79	0.26
41	1995 KJMA - Kobe UXUYUZ 100	0.36	17.88	1.24	0.09	1.11	4.66	0.85	0.28
42	1978 Tabas - Iran UXUYUZ 100	0.08	6.32	1.20	0.03	0.17	16.05	0.11	0.01
43	1978 Tabas - Iran UXUYUZ 100	0.10	8.52	1.60	0.05	0.23	12.22	0.16	0.02
44	1978 Tabas - Iran UXUYUZ 100	0.11	8.38	1.65	0.06	0.24	11.63	0.16	0.02
45	1978 Tabas - Iran UXUYUZ 100	0.24	15.69	3.24	0.11	0.49	10.83	0.56	0.09
61	1994 Sylmar - Northridge PEER XYZ ROT 60 CW	0.32	23.23	1.93	0.16	0.81	3.02	0.76	0.34
62	1995 KJMA - Kobe UYUXUZ 100	0.31	20.43	3.84	0.15	0.90	4.49	0.91	0.31
63	1995 KJMA - Kobe UYUXUZ 100	0.40	21.86	3.70	0.24	1.11	4.93	1.28	0.42
64	1995 KJMA - Kobe UYUXUZ 100	0.49	36.94	5.71	0.24	1.33	3.77	1.78	0.64
65	1995 KJMA - Kobe UYUXUZ 100	0.57	29.55	4.77	0.24	1.40	3.77	2.05	0.70

Table 6. Complete list of recorded (achieved) ground motions in z-direction during ST-2 (continued)

Motion No.	Name	PGA [g's]	PGV [cm/s]	PGD [cm]	Sa(T=1s) [g]	Sa(T=3s) [g]	D5-95 [sec]	Arias Intensity [m/s]	SIR [m/s^2]
66	1994 Sylmar - Northridge PEER rot 300 CW	0.27	11.44	3.49	0.24	0.27	4.53	0.29	0.09
67	1994 Sylmar - Northridge PEER rot 300 CW	0.35	19.55	2.63	0.32	0.31	4.27	0.52	0.19
142	1978 Tabas - Iran UXUYUZ 100	0.09	6.86	1.20	0.03	0.17	9.79	0.13	0.02
143	1978 Tabas - Iran UXUYUZ 100	0.14	9.69	1.67	0.06	0.28	11.49	0.18	0.03
144	1994 Sylmar - Northridge PEER UXUYUZ 100	0.25	8.09	1.33	0.18	0.32	3.67	0.23	0.08
145	1994 Sylmar - Northridge PEER UXUYUZ 100	0.08	2.98	0.51	0.06	0.12	4.23	0.03	0.01
146	1994 Sylmar - Northridge PEER UXUYUZ 100	0.15	4.83	0.90	0.11	0.19	3.46	0.08	0.04
147	1978 Tabas - Iran UXUYUZ 100	0.28	21.34	4.49	0.15	0.66	9.90	1.02	0.15
148	1994 Sylmar - Northridge PEER UXUYUZ 100	0.34	12.55	1.91	0.26	0.49	3.77	0.50	0.17
149	1995 KJMA - Kobe UYUXUZ 100	0.51	33.37	3.83	0.28	1.45	3.54	2.13	0.77
150	SinY T 200 6cycle	0.13	18.77	6.02	0.19	0.13	10.19	0.35	0.03
151	1995 KJMA - Kobe UYUXUZ 100	0.35	23.68	2.69	0.20	1.02	3.88	1.08	0.38
153	1978 Tabas - Iran UXUYUZ 100	0.18	12.68	2.59	0.09	0.38	11.28	0.33	0.05
155	1978 Tabas - Iran UXUYUZ 100	0.11	8.92	2.91	0.10	0.27	14.84	0.20	0.02
156	1994 Sylmar - Northridge PEER UXUYUZ 100	0.21	8.23	1.22	0.18	0.32	4.42	0.23	0.08
162	1978 Tabas - Iran UXUYUZ 100	0.27	21.44	4.39	0.15	0.66	9.49	1.09	0.16
163	1978 Tabas - Iran UXUYUZ 100	0.27	21.03	4.17	0.15	0.65	8.96	1.09	0.15
164	1978 Tabas - Iran UXUYUZ 100	0.26	22.58	4.62	0.16	0.65	8.96	1.08	0.15
165	1978 Tabas - Iran UXUYUZ 100	0.27	21.84	4.60	0.15	0.65	8.96	1.09	0.15
166	1978 Tabas - Iran UXUYUZ 100	0.17	12.05	2.38	0.10	0.38	10.44	0.33	0.05

One phone with no cover (Phone-6) was allowed to move freely on the shaking table during five, 1-D ground motions in ST-1. Three of these motions were sine-waves and two were realistic records from the 1989 Loma Prieta earthquake at Treasure Island and the 1999 Chi-Chi Taiwan earthquake at the TCU078 station). Subsequently, two phones (Phones 3 and 7) with different types of covers were allowed to move freely on the shaking table during four, 3-D earthquake scenarios in ST-2. All four motions were variations of the 1978 Tabas, Iran earthquake. As shown in Fig. 5, Phone-3 had a simple, sticky, plastic cover. Phone-7, on the other hand, had a glass cover with rubber pieces that provided considerable friction. Additionally, Phone-3 was allowed to fall in one event (trial 166) to study the response of a falling phone.

(a) (b)

FIG. 5. Photos showing the covers used on: (a) Phone-3; and (b) Phone-7 during four, 3-D earthquake scenarios in ST-2

2.1.4 Data Analysis and Results

The data collected during the shaking table tests was analyzed carefully to calibrate and quantify the response of the iPhone as a seismic sensor. A sampling rate of 100 Hz was adopted for the phones throughout these tests, while the high-quality reference accelerometers recorded data at 200 Hz. The ground motions recorded by seven iPhone and iPod touch sensors were compared with the reference in terms of acceleration-, velocity-, and displacement-time histories, Fourier Amplitude and Power Spectra of acceleration and velocity, Welch Power Spectra, Arias Intensity-time histories, and Acceleration Response Spectra to carefully document the differences.

During ST-1, the mean of four, high-quality, base accelerometer records was used as the reference signal in the direction of shaking. Two sets of high quality accelerometers in three orthogonal directions were mounted rigidly on the platform during ST-2, the records of which were averaged for each direction, respectively. For proper comparison, the sampling rate of the reference signals was reduced from 200 Hz to 100 Hz (using the decimate function in MATLAB with proper filtering). All the records were cross-correlated and shifted in time for better comparison.

The time-steps were not uniform in phones and appeared to fluctuate slightly. The standard deviation of the phone time-steps ranged from 3% to 8% of the mean time-step. Importantly, the iPhone periodically missed a sample point. The jitter in the time-step appeared to be related to increased processing on the iPhone, leading to irregular time-slicing and hence, more variability in the time-step (as shown in Fig. 6). As such, the mean time-step throughout the record was used as a constant time-step for further analyses. Modifying the timesteps to be uniform had a negligible effect on the spectral properties of the signals because of the relatively small jitter in the signal. Following these changes, the phone and reference signals were base-line corrected, zero-padded, and band-pass filtered at corner frequencies of approximately 0.2 Hz and 25 Hz with a 3rd order, acausal, butterworth filter.

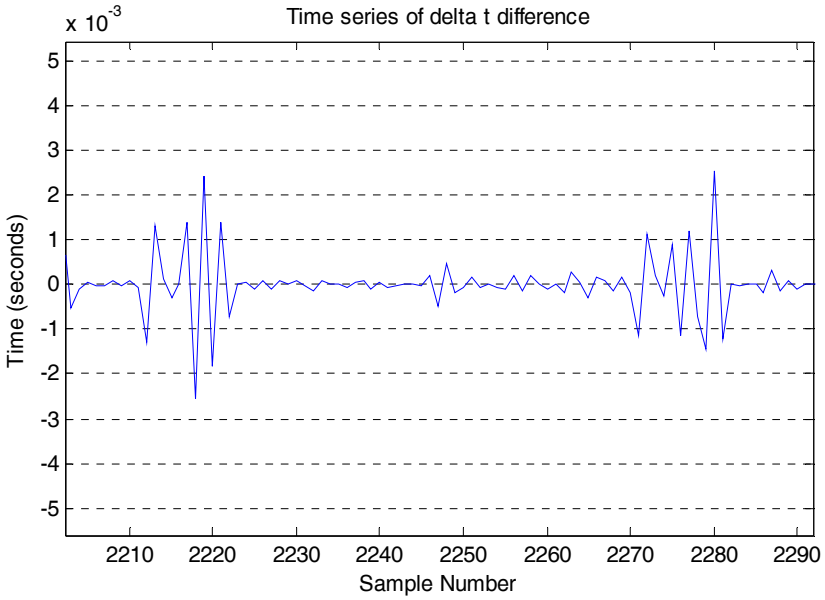

FIG. 6. Example of time-step variations with time in iPhone records

2.1.4.1 Non-moving (Stationary) Phones

The results obtained during 75 one-dimensional input ground motions in ST-1 are included in Appendix A. All phones were rigidly mounted to their holders during these shakes and independent phone movements were negligible. These figures compare the response of seven iPhones and iPod touches with those of the reference accelerometer in terms of acceleration-, velocity-, and displacement-time histories, Fourier Amplitude and Power Spectra of acceleration and velocity, Welch Power Spectra, Arias Intensity-time histories, and 5%-damped Acceleration Response Spectra. The presented comparisons show promise in the quality of phone recordings. The phones performed well in terms of estimating spectral accelerations, *PGA*, *PGV*, and *PGD* for most ground motions. Peak Ground Velocity (*PGV*), which is a good indicator of damage, is captured reasonably well. In general, iPhone and iPod touch sensors showed a tendency for slightly over-estimating the ground motion energy and hence, Arias Intensity (I_a). Even though a comparison of individual iPhone acceleration response spectra with the reference was not ideal, the averaged spectrum of the seven phones compared well with that

of the reference. These observations are helpful in evaluating the response of the entire phone local array as a seismic sensor.

The results obtained from 36 input ground motions in ST-2 are provided in Appendix B. Similar comparisons are made between the records obtained from seven iPhones and iPod touches and those from high-quality accelerometers. In general, the comparisons between the records obtained from the phones and the reference accelerometers in both time and frequency domain became slightly worse during ST-2. This might have been due to damaged accelerometers after a large number of intense shaking events. More importantly, the response of the entire phone as a seismic sensor is more complex during a 3-D motion, which influences its recorded signals. Nevertheless, the comparisons were acceptable in an average sense, particularly in terms of spectral accelerations.

Based on previous studies (e.g., Joyner and Boore 1988), the response spectral values and other earthquake intensity parameters, such as the Arias Intensity, were assumed to be log-normally distributed. Hence, the logarithms of the earthquake intensity parameters were used to compare the phone and reference records. The errors in the intensity parameters recorded by phones during all shaking events compared to the reference signal are presented as a function of various properties of the input ground motion during ST-1 and ST-2 in Appendices C and D, respectively.

Motions recorded in three orthogonal directions in a given trial during ST-2 are presented as separate ground motions in these plots. The horizontal and vertical components of the acceleration-time histories were not combined in a resultant vector, because they tend to have very different characteristics during an earthquake motion. These plots show that the errors in the phone-estimated intensity parameters appears to depend on some of the characteristics of the input ground motion, particularly its Peak Ground Acceleration (*PGA*) and Arias Intensity (I_a). The error in most intensity parameters appears to decline for stronger ground motions. As an example, Fig. 7 presents the errors in the log of the phone recorded Arias Intensity parameters as a function of the *PGA* of the input ground motion during ST-1 and ST-2. These results indicate that the error in the phone recorded Arias Intensity sharply decreases for stronger ground motions with larger *PGA*'s (particularly during 1-D shaking in ST-1, Fig. 7a). With the available data, these errors can be statistically evaluated based on key input ground motion properties. A parametric study of these errors will lead to better estimates of key ground motion parameters from a cluster of low-quality phone records.

The accuracy and consistency of the acceleration-time histories recorded by individual phones may be estimated using a system parameter method proposed by Baise and Glaser (2000. In this method, the accuracy of the phone in measuring accelerations may be quantified by the mean value of the squared error term (*MSE*), normalized by the maximum amplitude of a ground motion (e.g., *PGA*, *PGV*, *PGD*, etc.). The *MSE* for a given phone record during a given trial may be computed as:

$$MSE(acceleration_{phone}) = \frac{\sum_{i=1}^{N}[a_{phone}(t_i) - a_{reference}(t_i)]^2}{N} \quad (1)$$

where a_{phone} and $a_{reference}$ are the acceleration-time histories recorded by a phone and the reference instrument, respectively; and N is the number of time indices in a given record. The *MSE* is an overall measure of the error magnitude for a phone acceleration measurement, which is a better indication of the error than the error in an individual intensity parameter derived from the recorded acceleration-time histories.

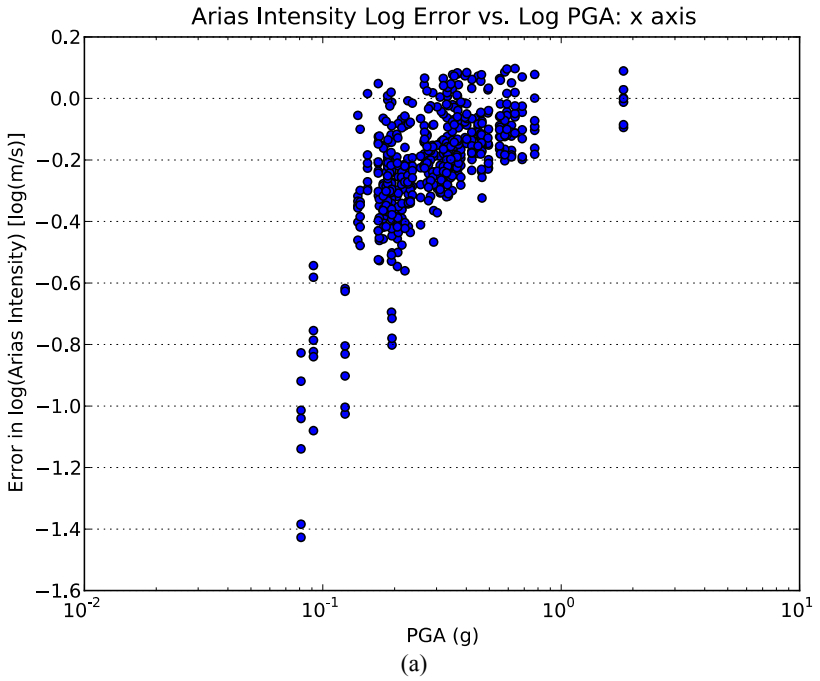

FIG. 7. The error in the log of the Arias Intensity of phone records with respect to that of the reference accelerometer versus the *PGA* of the input motion during: (a) ST-1; (b) ST-2 in the x-direction

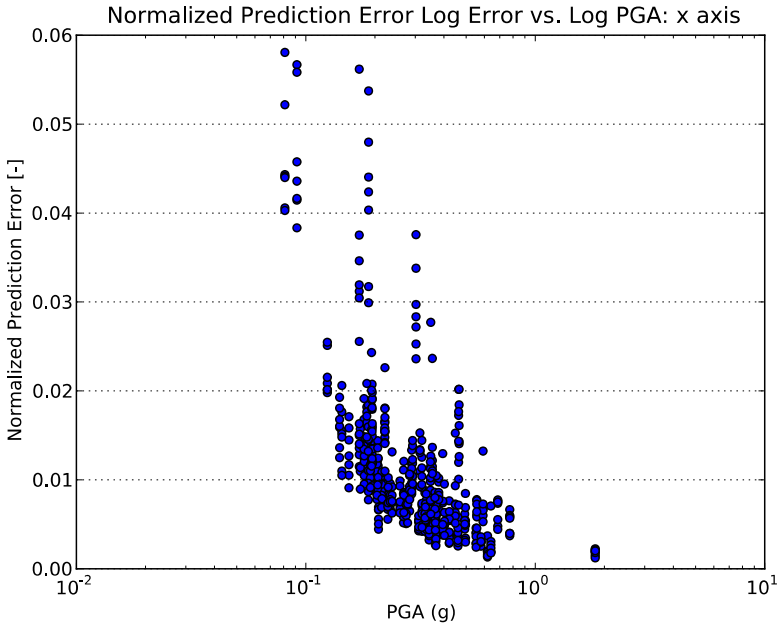

(a)

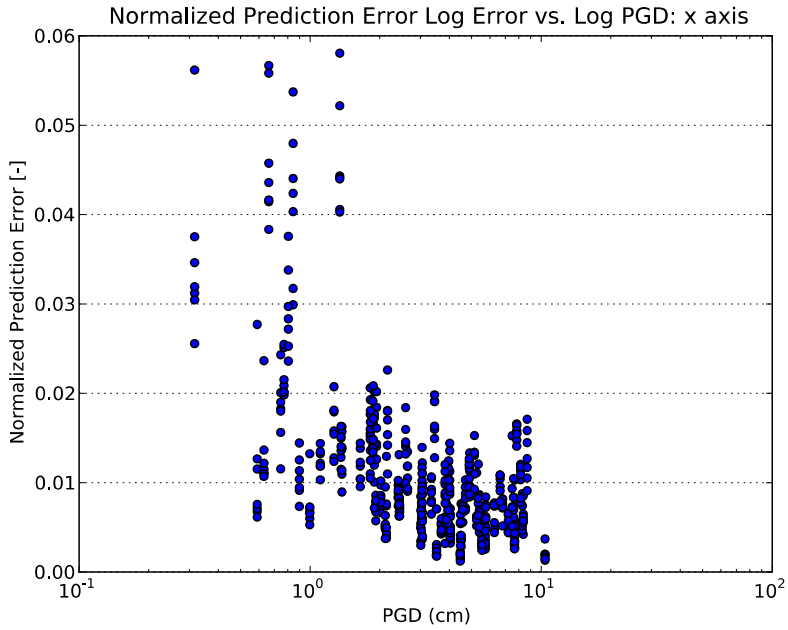

(b)

FIG. 8. The *NPE* of phone records during ST-1 as a function of: (a) the *PGA*; and (b) the *PGD* of the input motions

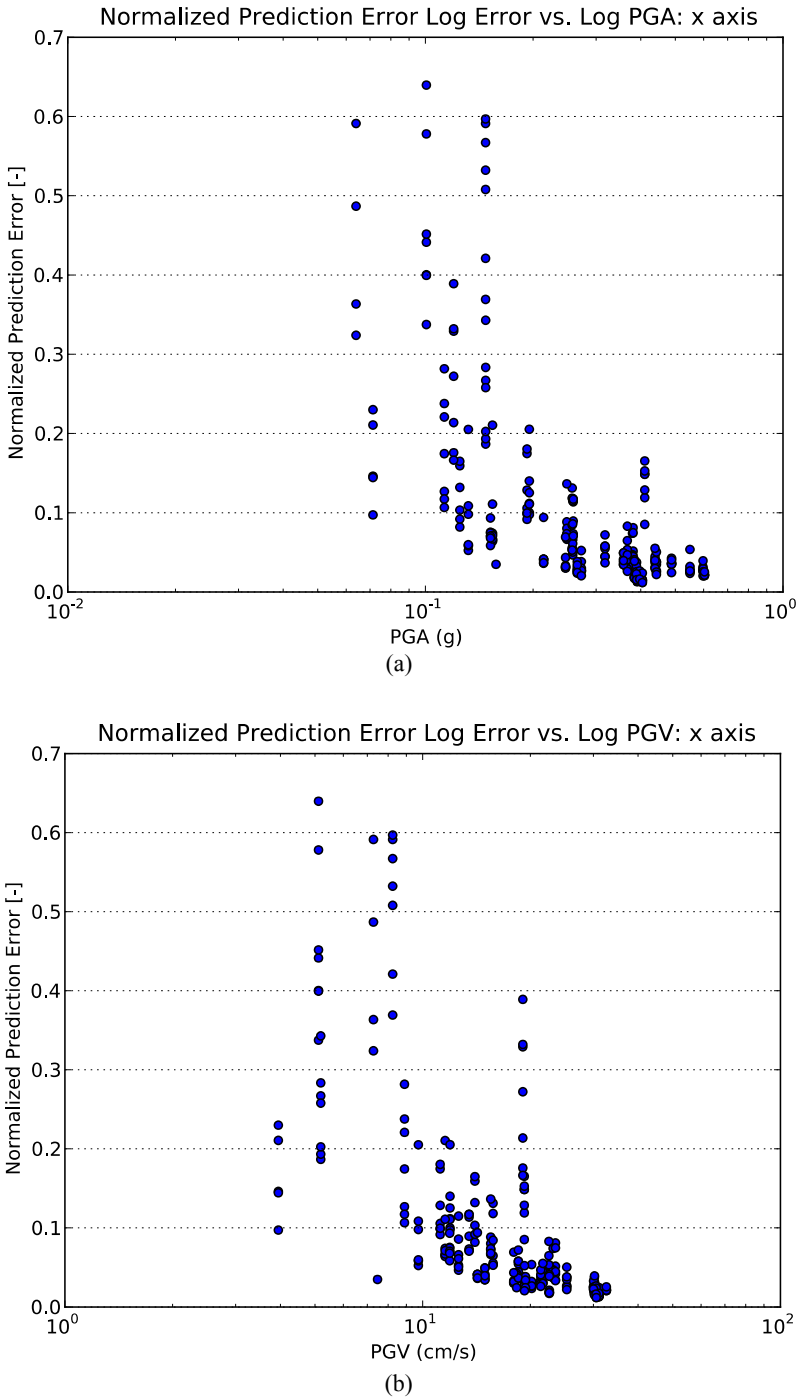

FIG. 9. The *NPE* of phone records during ST-2 in the x-direction as a function of: (a) the *PGA*; and (b) *PGV* of the input motions

Because the earthquake acceleration-time histories are non-stationary, the *MSE* is likely non-stationary as well (Baise and Glaser 2000). Therefore it is necessary to specify the portion of the earthquake motion that is to be analyzed for computing the error with the assumption of a constant mean. The time window of the ground motions with peaks that exceeded 0.2(*PGA*) was used in these calculations. The Normalized Prediction Error (*NPE*) was subsequently estimated for each phone by dividing the *MSE* by the square of the *PGA* of the corresponding motion. The *NPE* is a useful statistical tool with which to quantify the goodness of a phone measurement. Fig. 8 presents the calculated *NPE* values for each phone during different trials in ST-1 with respect to the *PGA* and Arias Intensity (I_a) of the input motion. Fig. 9 shows similar plots for the *NPE* of the data obtained from ST-2 with respect to the *PGA* and *PGV* of the input motions. Both tests showed a strong correlation between the *NPE* of the phone records and the intensity of the input motion: the errors reduced sharply for stronger ground motions.

The "goodness-of-fit" between the 5%-damped acceleration response spectra obtained from the phones and the reference accelerometer was quantified using the statistical evaluation procedure developed by Abrahamson et al. (1990) in terms of phone's bias and uncertainty. For a given model, the residual, *r*, was calculated as:

$$r_{im}(f_k) = \log S_{Aim}^{ref}(f_k) - \log S_{Aim}^{phone}(f_k) \tag{2}$$

where $S_{Aim}^{ref}(f_k)$ and $S_{Aim}^{phone}(f_k)$ = the spectral ordinate of the reference and phone recorded motion, respectively, as a function of frequency, f_k; i = earthquake index; k = frequency index; and m = component of motion. The bias (or mean of the residuals) was calculated at each frequency, f_k, as:

$$bias(f_k) = \frac{\sum_{i=1}^{N_i}\sum_{m=1}^{N_m} r_{im}(f_k)}{N_i.N_m} \tag{3}$$

where N_i = number of earthquake events; and N_m = number of components of motion. The variance in the error term (phone variance) and the standard error of the bias were then calculated as:

$$\sigma_{phone}^2(f_k) = \frac{\sum_{i=1}^{N_i}\sum_{m=1}^{N_m}[r_{im}(f_k) - bias(f_k)]^2}{(N_i.N_m) - 1} \tag{4}$$

$$\sigma_{bias}(f_k) = \frac{\sqrt{\sigma_{phone}^2(f_k)}}{\sqrt{N_i.N_m}} \tag{5}$$

The bias in the acceleration response spectra obtained from stationary phones during ST-1 and ST-2 is plotted in Fig. 10. As shown in equation (3), these plots combine the bias of each individual phone during all the input ground motions in a given experiment as a function of frequency or period. The bias shown in Fig. 10b only combines the horizontal components of the input motions in ST-2, in order to separate the effect of the vertical motions with different characteristics. These plots indicate that the bias is sufficiently low during the period range of interest for most engineering applications (about 0.1 to 1 sec) in both experiments, although the bias reduced significantly during the 1-D earthquake scenarios of ST-1.

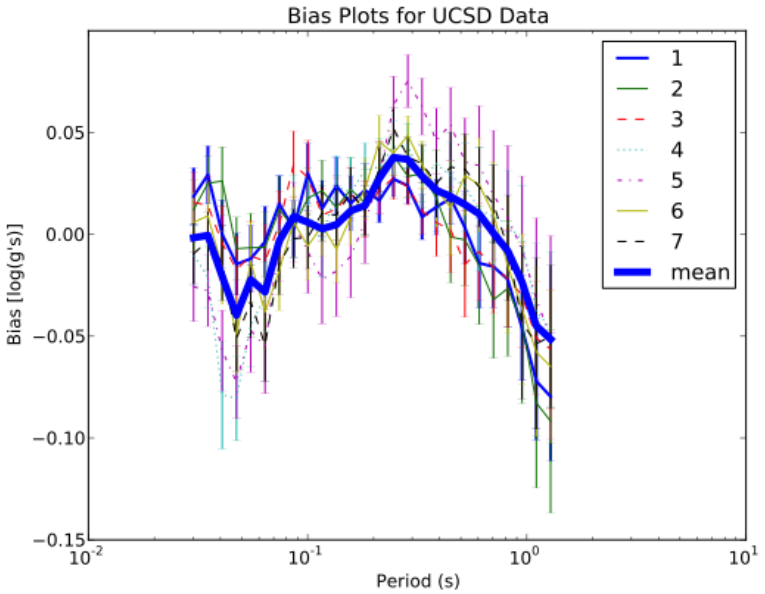

(a)

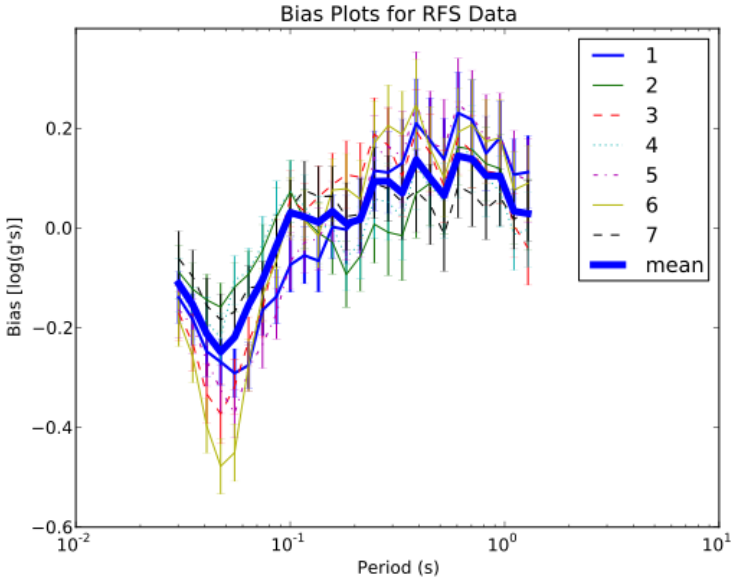

(b)

FIG. 10. Bias in the 5%-damped acceleration response spectra recorded by 7 iPhone and iPod Touch sensors during: (a) 1-D shaking in ST-1; (b) 3-D shaking in ST-2, where the horizontal components of the motion were used in calculating the bias

2.1.4.2 Moving and Falling Phones

One phone with no cover (Phone-6) was allowed to move freely on the shaking table during five, 1-D ground motions in ST-1. The results obtained from these shakes are included in Appendix E. The input motions were one-dimensional. However, since the phone was allowed to move and rotate freely on the table, the resultant of the two horizontal phone accelerometers appeared to yield the best comparison with the reference record. The acceleration amplitudes recorded by the moving phone were largely under-estimated during the sine-sweeps due to the

displacement of the phone. However, the frequency of the sine-waves was captured well. The comparisons improved substantially during realistic ground motions with a wide range of frequencies and amplitudes. The results were particularly improved for spectral accelerations. These comparisons show promise in attaining reasonable estimates of ground motion intensity from phones left free to move on a flat surface during earthquakes, even with no cover.

Subsequently, two phones (Phones 3 and 7) with different types of covers were allowed to move freely on the shaking table during four, 3-D earthquake scenarios in ST-2. As was shown in Fig. 5, Phone-3 had a simple, sticky, rubber cover. Phone-7, on the other hand, had a glass cover with rubber pieces that provided considerable friction. Additionally, Phone-3 was allowed to fall in one event (trial 166) to study the response of a falling phone. The results obtained from these shakes are included in Appendix F.

As expected, the comparisons were significantly improved for phones with sticky covers compared to those without any cover. Phone records compared reasonably well with the reference in these tests, as Phones 3 and 7 did not show noticeable independent movements on the table during such intense shaking events. The use of a frictional glass cover on Phone-7 was particularly successful in minimizing the amount of sliding on the shaking table. The acceleration amplitudes recorded by Phone-3, however, were slightly under-estimated due to its minor tendency to slide on the table during shaking.

Phone-3, which was allowed to fall during trial 166, showed a spike in frequencies ranging from about 0.2 to 0.5 Hz mostly in the y and z direction. This acceleration spike was also evident as a sudden increase in the corresponding Arias Intensity-time histories at the time of falling (e.g., Fig. 11). The comparisons of the recorded time histories in the y and z directions were largely unacceptable, but the sudden increase in the value of Arias Intensity may be used to detect the falling instruments and remove the signal. It must be noted, however, that the accelerations in the x-direction compared well with the corresponding reference during this event. These observations provide valuable insight into the response of moving and falling phones that need to be detected and analyzed.

2.1.4.3 Performance of Client Application and Server

These shaking table tests also provided an opportunity to test the performance of the pilot iShakeTable mobile phone software (shown in Fig. 2). When wireless connection was maintained, the process of data recording, storage, and transmission was carried out successfully. Multi-tasking is not allowed on iPhone models older than version 4.0. Hence, an alarm, text message, or a phone call may interrupt the successful and continuous running of the application. For successful testing, the "airplane" mode was manually turned on to prevent third party activities from interrupting the application. This problem is largely addressed in recent iPhone and iPod touch models. With the introduction of iPhone Operating System 4.0, all compatible iPhones have background activity capabilities. Receiving alerts such as text messages or phone calls will not longer disturb the application.

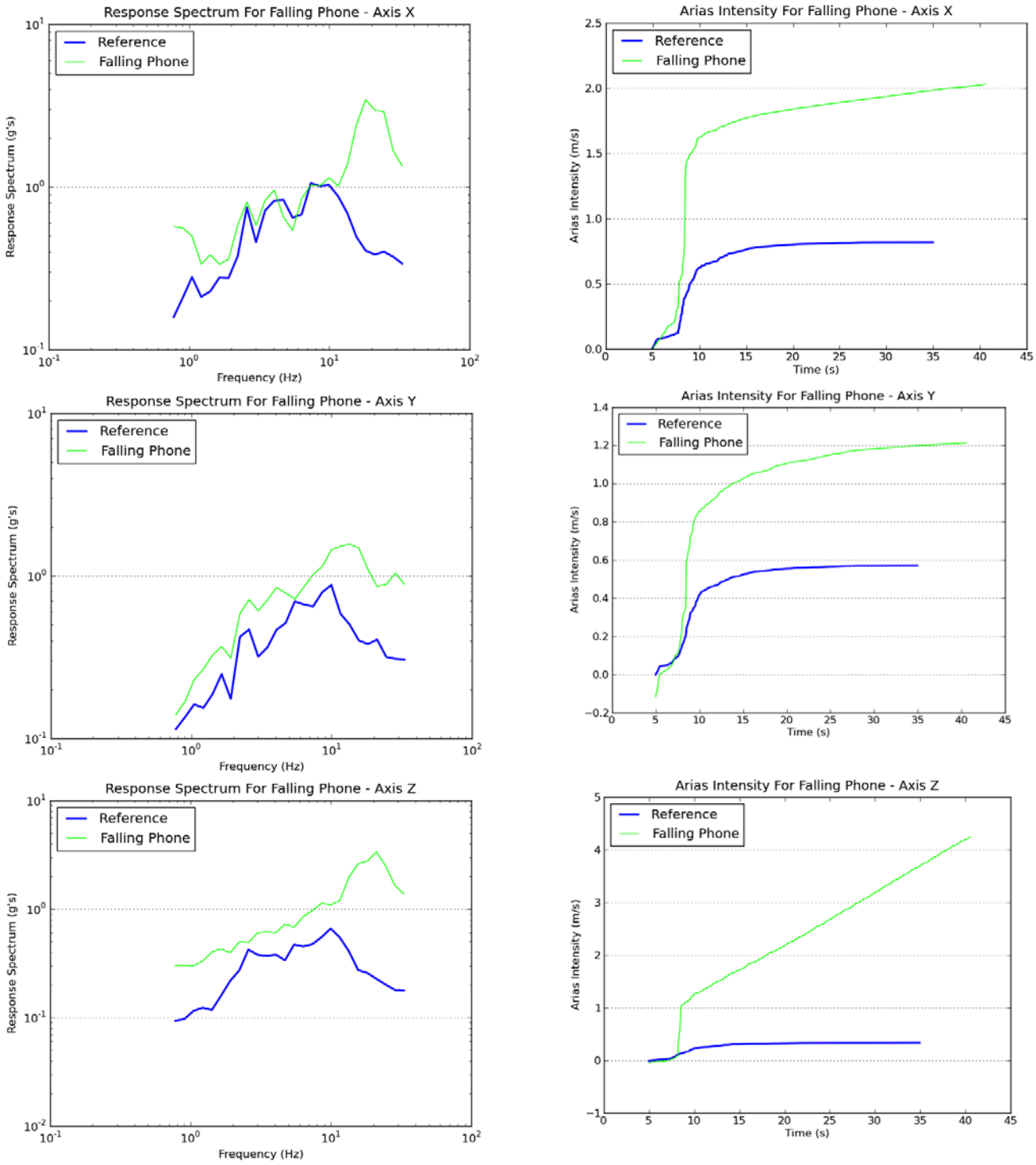

FIG. 11. Acceleration response spectra (5% damped) and Arias Intensity-time histories of the falling phone in comparison with the reference instrument in different directions

2.2 Testing of Phone Connection

2.2.1 Uncertainty in sensor state

One drawback from remote sensing is the inability to strictly monitor the environment of the measurement, of which fixed stations have the luxury. For the iShake project, the actual ground motion is sought after, but factors such as building response, orientation of phone, and the rigidity of the connection of the phone to the surface of contact obscure the signal. If the actual state of the sensor was known, signal processing techniques and filtering could be applied to the signal to recapture some characteristics of the pure signal. To these ends, the following is a proposed model for classifying the connection of a phone to its surface as either rigid or loose, in order to properly process the measured response.

2.2.2 Model for Sensor State Classification

2.2.2.1 Model Input

For the purposes of this model, there is assumed to be a "reference" ground acceleration signal with which to compare other signals. This is a realistic assumption, as high-quality recordings of earthquakes are often available from the strong-motion stations of government agencies, such as the United States Geologic Survey (Wald et al 1999).

The base input into the model is the three-dimensional accelerometer recording from the iPhone for a given shaking event (the orientation is assumed to be known, so magnetometer data may be discarded). The acceleration time-series is then characterized by a set of statistical parameters:

1. Peak Ground Acceleration
2. Peak Ground Velocity
3. Peak Ground Displacement
4. Spectral Response at .3 seconds
5. Spectral Response at 1 seconds
6. Arias Intensity
7. The Shaking Intensity Rate (SIR)

Using the reference signal mentioned before, the absolute error is obtained for all of the above parameters. It is the relative distribution of these errors parameters that are used as input into the classification model.

2.2.2.2 Graphical Representation

The graphical relationships are represented in Figure 12. For each shake event recorded, three signals are produced: one for each axis of translation of the sensor. This means that there are three sets of parameters to act as input into the model, labeled as the observed θi nodes in Fig. 12.

Taking a single axis, the likelihood that that specific axis is loose or rigid is then calculated. The error parameters are assumed to be normally distributed, leading to a multivariate

Gaussian distribution for a set of parameters on an axis. The covariance matrix and mean vector is determined from a training set of shakes that are labeled as either loosely or rigidly connected. The mean and covariance matrices are computed using standard statistical software packages, which maximize the likelihood of the input training data.

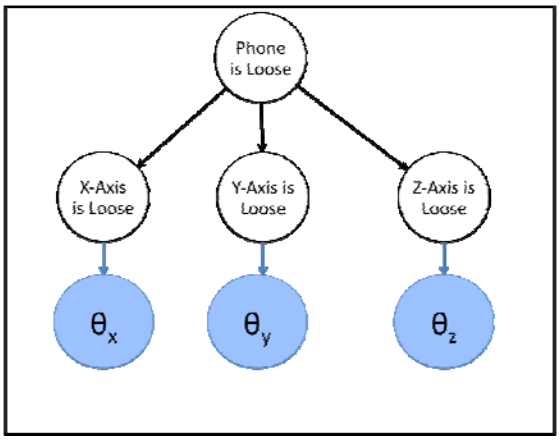

FIG. 12. Graphical representation of the connection-type prediction model, where θi represent the measured error parameters for axis i

From these estimated parameters, the likelihood of the axis of a phone being loosely connected is calculated as follows:

$$\mathbb{P}[\text{Axis i is loosely connected}|\theta_i] = \frac{f_{\mu_l,\Sigma_l}(\theta_i)}{f_{\mu_l,\Sigma_l}(\theta_i) + f_{\mu_r,\Sigma_r}(\theta_i)} \tag{6}$$

which acts as the relative weight of the loose likelihood compared to the rigid likelihood. This calculation is repeated for all three axes to obtain a likelihood value for each axis from the signal. The final classification is then inferred from the three axial likelihoods. Utilizing the generalized linear model framework, the distribution is assumed to be logistic (z), where z is obtained through a linear combination of the axial likelihoods. The logistic function suits the situation well, as we have three predictor values in the axial likelihoods, and a binary outcome dependent variable (looseness) to which we map. The looseness likelihood of a recording conditioned on axial likelihoods is as follows:

$$P[\text{phone is loose}|x] = \frac{1}{1 + \exp(-z)} \tag{7}$$

$$z = \beta_0 + \sum_{\text{axis } i} \beta_i x_i$$

where xi is the axial likelihood for axis i, and β represents the linear coefficients for the GLIM model. Using the GLIM framework, the β parameters are inferred from an iterative method, such as the iterative recursive least-squares method (which is used in this paper) (Bohning 1992). The

same training set is used to calculate the beta parameters, by first calculating axial likelihoods for a given signal, then inferring β from these values.

Finally, we have a process for computing the likelihood of a phone being loose:

1. Parameterize test signal and reference signal into input error parameters PGA, PGV, PGD, etc.
2. Calculate all three axial likelihoods from error parameters
3. Calculate likelihood from logistic distribution of axial likelihoods

The end result is an estimation of the probability that the given signal was produced by a loosely connected phone. Classification is now a matter of setting a decision factor on the likelihood.

2.2.3 Testing Configuration

Figure 13 depicts the testing station for data collection. There are 5 iPhones oriented identically on the table, with translational motion fixed by the constraints on the shaking table. The program works by inputting some testing parameters (trial number, loose or rigid, phone name), then controlling the accelerometer recording through the start/stop buttons on the application. All phones start and finish recording a trial at roughly the same times. Then the signals are all transmitted (with their proper tagging for looseness and trial number) to a server for parsing, storage and first-order processing. First-order processing is necessary for such factors as time-step uniformity and time-synchronization. The server now provides us with the raw acceleration signals, ready for manipulation.

FIG. 13. A photograph of testing setup, with Loosely connected and rigidly connected iPhones on the same shaking surface

The concept behind the testing was to establish one rigidly-attached phone per trial as a reference accelerometer, and serve as the base-measurement to calculate error values. Then, a different assortment of rigidly-attached and loosely-attached iPhones were also included in the trial. When a trial begins, the phones will begin recording and a shaking event is imposed. Finally, the trial will be transmitted to the server, with the proper labeling of the states of the phone for the given trial (loose or rigid).

This process was repeated 20 times for the training set and 10 more times for the testing set. To remove such factors as specific-phone bias and phone-location on table, the phones were rearranged, and reference accelerometer duties alternated between all the phones. The hopes of

these measures were to eliminate the possibility that the tests were isolating hidden variables, such as site-specific responses on the testing table to shakes.

The end result of the testing was a set of loose phone errors and rigid phone errors for a number of phones over a number of trials. The training set gives the needed information for determining the parameters for the multivariate distributions over the axis-specific input error parameters, and the logistic distribution parameters over the axial likelihoods.

2.2.4 Results and Analysis

2.2.4.1 Parameter Estimation

The trials ran from the testing are split into two sets: training data and testing data. The training data was run to calculate model parameters as described in Section 2.2.2 Then, the training data was rerun to get classification predictions. The results are shown in Fig. 14.

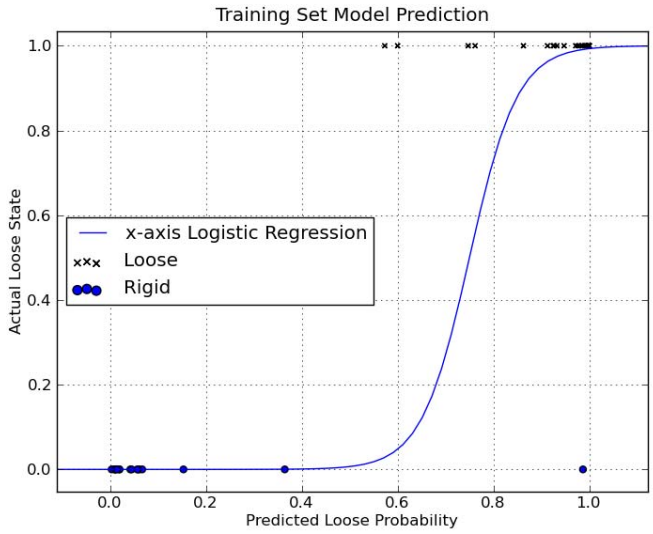

FIG. 14. Plot of data used to train the model (Note: most of the data points are clustered at the tails with a few outliers)

The figure shows a very good prediction dichotomy of the sample points, with only one overlapping point (a false positive). To test whether or not the model was fitting intricacies of the specific data-set, the model is run against a test data set, that was not used for training the model.

2.2.4.2 Test Data Set and Classification Results

The results from Figure 15 show the same true confirmation properties of the training set, as 95% of the loose phones were reported as loose. What differs is the number of false positives

reported by the model, as there was only one false positive from the testing set, but half of the rigid testing set was also reported as loose (assuming an acceptance level of 75%).

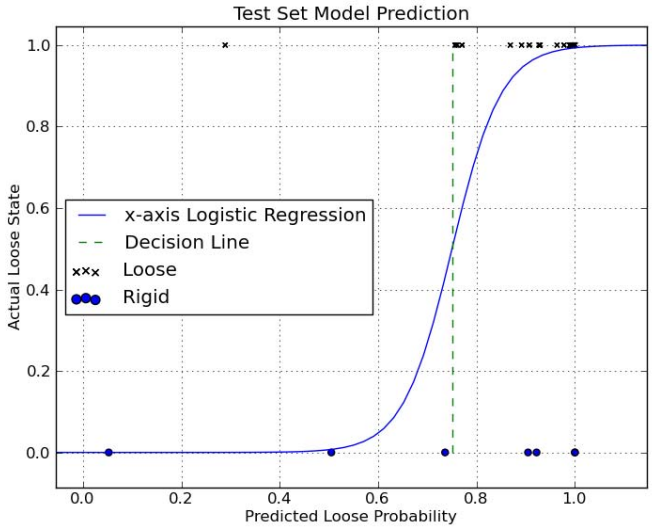

FIG. 15. Plot of test set: choosing a decision line of 0.75 will correctly classify almost all loosely connected phones, but will also introduce a number of false positives

There could be a number of reasons for the reporting of false positives. The most obvious reason for these results would be improper restraining of the rigid phones to the table. Also, due to the proximity of the phones and response of the table, there may be localized effects of shaking that were not captured by all phones during the trial. Obviously, another possibility for the larger error is the relatively small sample size for the testing set.

3 SYSTEM REVIEW

3.1 iPhone as a Seismograph

While the iPhone is not technically designed to be a scientific sensor, the addition of inexpensive, low-quality sensors into the device permits the exploitation of the device for such a use. The addition of the accelerometer into a mobile phone allows one to treat the phone as a means of sensing ground motion data, along with the a means of transmitting the data to a central system. Thus, the iShake Project sets out to utilize the iPhone as a mobile sensor for seismic data.

3.1.1 Hardware Components and Capabilities

The essential component of the iPhone for seismic data sensing is the accelerometer. The accelerometer is able to capture the acceleration-time history of the phone, and all other

important seismic parameters can be estimated from this data. The iPhone 3GS has a STMicroelectromechanics LIS331DL 3-axis MEMS accelerometer, with a sampling frequency of 100 Hz and an accuracy of roughly 0.02 g. Since any frequencies greater than 50 Hz is not of interest in earthquake engineering applications, the sampling frequency of the phone is sufficient. Since the phone accelerometer has 3 axes, it is able to record all accelerations in three dimensions.

3.1.2 Phone Location and Orientation Determination

In addition to the accelerometer, the iPhone includes a 3-axis magnetometer, which acts as a compass in common use, and a GPS unit for geo-location and navigation.

For a traditional seismic recording, the orientation and location of the seismograph is constant and known. These parameters are dynamic for the iShake project and the orientation of the phone and its location are desired to be determined and associated with any data that the accelerometer reports. Knowing the location and orientation of a record is critical, as the three axial accelerometer recordings must be put in a global reference frame. Using the accelerometer, magnetometer, and GPS readings, the orientation and location of the phone can be estimated.

The location (latitude and longitude) of the iPhone is readily available from the GPS estimate. Even when a GPS reading is not available, the iPhone can use the local wireless internet connection to estimate its location, which has an acceptable accuracy (e.g., 10-100 meters) in most cases. The orientation estimate must use all three sensors, along with the assumption that the phone is relatively stationary. When the phone is still, the reading from the accelerometer is strictly the force of gravity on the sensor. Based on this assumptions, two of the three angular coordinates may be determined, while a final coordinate remains unknown. It must be noted that rotating an iPhone while keeping it flat on a desk will have no effect on the stationary gravity measurement. To obtain the last coordinate, we may consider that the Earth's magnetic field can be estimated given the phone's geo-location and the current time. The magnetometer records the surrounding magnetic field. Assuming that the local magnetic fields are small, the magnetometer will record the earth's magnetic field at its current position and time. The end result is that the iPhone has two reference vectors (gravity and the Earth's magnetic field) to which it can compare its own measurements. Utilizing the Triad algorithm (Black 1964), which is classically used to estimate an aircraft's yaw, pitch, and roll in aerospace engineering, the three absolute angular coordinates can be estimated for any position. This information may be used to give the local phone accelerometer readings a global meaning.

3.2 System Architecture

Figure 16 provides an overview of the iShake system architecture. The following sections describe the components of the iShake system, consisting of the phone, server and database, earthquake notification, and data visualization.

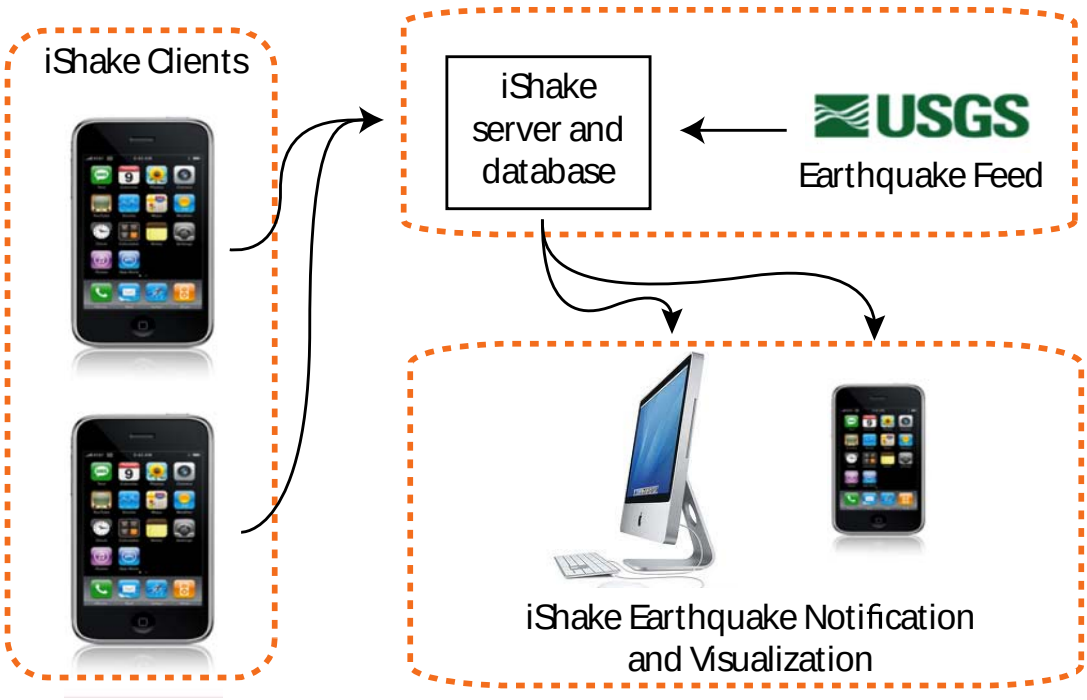

FIG. 16. Overview of the iShake System

3.2.1 Phones as Clients

The iPhone can best be modeled as an intelligent sensor that has the ability to transit its data. By approaching the system in this manner, the iPhones create a spatially-varying grid of wireless sensors. Thus, the required pieces of information from the sensor to uniquely describe its state, in addition to the acceleration data, are the timestamp, the geo-location, the phone's orientation, and a unique phone identifier. The phone identifier data becomes important for learning the tendencies of individual phones to overestimate or underestimate certain parameters.

3.2.2 Data Aggregation For Similar Events

When the seismic data is received by the server, the data consists of a large number of independent events with no explicit relation to one another, as if hundreds of local and independent shakes caused the triggering of transmission of the data from the clients. The server can relate the individual phones to one another by creating a global shake event and assigning the individual phone events to the newly created global event. After assignment, the individual events sent to the server may be viewed as a large collection of similar events, each event capturing a unique component of the ground motion due to its location, timestamp, and other environmental factors.

3.3 Application Development

The goal of using an iPhone in the iShake Project is to treat it as a passive sensor. As a result, the iPhone application has the unique property that it has little to no human interaction or input. Additionally many important processes do not take place visually. The goal of the application is to achieve full sensor functionality while providing minimal user interface. Since these two components of the app are largely independent, the focus of the discussion of the application will be on the background sensing.

3.3.1 Program Flow

There are two important components to the design of the program flow. First, the iPhone must achieve a steady state before it can start sensing in order to determine the orientation of the phone and to signal that the user is not manipulating the phone and hence, the phone is in a passive state. Second, the vast majority of the time the application is in use, it will be in the passive mode, waiting for an event to record and transmit.

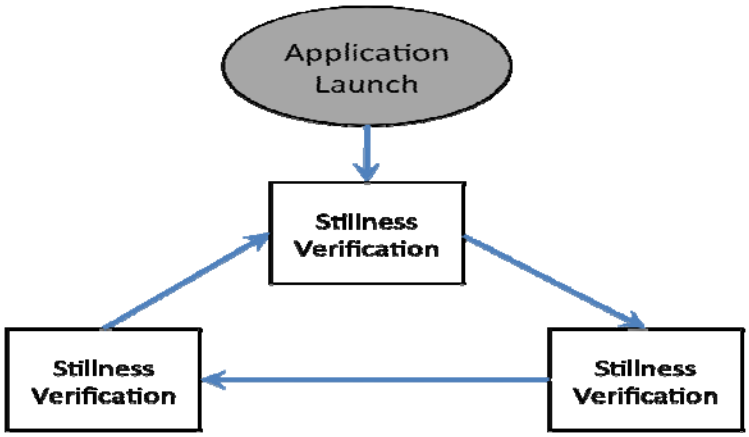

FIG. 17. iShake Application Flow Diagram

These components of the application create three distinct states for the application (Fig. 17):

1. Wait For Stillness - the application has either just been launched or experienced a period of large shaking and hence, it must determine its orientation and guarantee that it has returned to a passive state.

2. Passive/Buffer Mode - the application has achieved a passive state and is waiting for an event to trigger it. A time history of a set amount of time must be kept, but no data is transmitted during this state.

3. Streaming Mode - an event has triggered the iPhone to leave the buffer state and start streaming its data to the server for a set amount of time. In addition to streaming the immediate record post-triggering, the buffer history is also sent to the server to provide a more complete time history of the ground motion.

3.3.2 Verifying the Phone's Stillness

There are two components considered for an iPhone's stillness: a maximum cumulative amount of movement for a period of time, and a maximum permitted single movement value during the same period. To implement the cumulative movement calculation, a definition of movement must be created. For this implementation, the movement for time T is considered to be the difference in accelerometer readings from time $(T - \delta t)$ to T, where δt is the time step for each acceleration reading. The cumulative sum of the movements is taken for a time period. In addition, no single movement value during this time period may exceed some maximum allowable movement value, regardless of the cumulative sum value. If both of these conditions are satisfied, then the iPhone is classified as still, and continues to the next state. If either condition fails, then the iPhone stays in this state indefinitely, waiting for the conditions to be satisfied.

3.3.3 Passive/Buffer Mode

Once the state of the iPhone is classified as still, it immediately begins recording on all sensors (accelerometer, magnetometer, and GPS). A predetermined buffer period is given for the state, instructing the phone on how long of a history it should always keep in memory, while discarding any data older than the buffer period. The implementation for this buffer is a First In, First Out (FIFO) queue, that will remove the oldest entry in the queue from the front and add the newest entry to the back of the queue. This process continues until a threshold acceleration is reached, which then sets of a trigger, and signals the iPhone that a shaking event is now occurring.

A record buffer is necessary to capture the p-wave of an earthquake event. The time of both s-wave and p-wave arrivals are important in an acceleration record to adequately locate the epicenter of an earthquake event. P-waves are the first waves to reach an area and are often less intense than the following S-waves. Because of their relatively low intensity, the p-waves are often not strong enough to trigger the iShake streaming mode. Thus, always recording a set period of time before a triggering event is necessary to capture all relevant information from a seismological event.

3.3.4 Streaming Mode

After triggering occurs, the iPhone begins the transmission process. The buffer history from the previous mode is the first set of data to be transmitted to the server. While the iPhone is constantly recording new data from the sensors, it will also transmit periodically to the server to maximize the data received by the server immediately following a large earthquake event before communication lines go down. The oversaturation of communication networks following a major disaster that is spatially concentrated is typical. After the total transmission time has transpired, the iPhone will return to verifying the stillness of the phone and recalculating its orientation, thus completing one event cycle.

In the case of any transmission failure, the block of data associated with the failed transmission is stored, along with any relevant state information, which will be placed in a delivery queue later for retransmission.

3.4 Server Development

The server for the iShake project acts as the administrator for the possibly large number of events being sent from the iShake clients. Due to the variable nature of the transmitted events (time drift, false events, geospatial variability, phone orientation, phone type, etc.), different levels of classification of events must be made. The server handles incoming requests from clients, then classifies and stores the data from the requests based on aforementioned variables.

3.4.1 Description of Shake Event

There are large amounts of independently collected data being transmitted to the server. To make sense of this data, a model was developed to store data efficiently and to make sure that all records can be uniquely linked to a specific event sent from an iPhone. The term "shake event" describes all the data related to a specific phone, transmitted from a single cycle of the application shake cycle (a single passing of the Streaming Mode state). To further classify this event, the starting date and time, the phone type (i.e., iPhones and iPod Touches at this time), and the unique phone ID is stored with this data.

3.4.2 Shake Event Verification

Although any data transmitted from the iPhone is considered a shake event, we may reasonably assume that most events sent by the phone will not actually correlate to a real earthquake event. Thus, when shaking events are first received by the server, the event is classified as "unverified".

In order to verify or reject a shake event, all unverified events are compared against a database of recent earthquake events reported by the USGS, made available to the public through an online xml feed. Since the iShake project is designed for California earthquakes at this time, this verification process is considered to be acceptable. After a certain amount of time, the event is checked to fall within a certain radius and time period of all recent USGS earthquake events. If an event is verified, it is associated with the matching USGS earthquake event and is then clustered with all other iPhone shake events that were also associated with the same earthquake. All events that are not associated with an earthquake are classified as "rejected" at this time and are considered to be a false event. We are currently keeping these false events to better understand the signal characteristics of false events.

3.4.3 Signal Processing

The accelerometer readings from the iPhone do not accurately represent the motion experienced by the ground directly in contact with the iPhone. This is becuase the phone is not rigidly connected to the ground, the accelerometer is housed inside the iPhone that introduces its own influence on the signal, and other environmental factors when the shaking event occurred. To attempt to obtain a better estimate of the actual ground motion, the accelerometer data must be processed. While some processing may be done directly on the phone (such as a low pass filter to remove high frequency noise), other processing must take place on the server. If an earthquake event has unusually high or low frequency components, then filtering of such an event would be conscious to preserve the low frequency activity.

In order to properly deal with clock-drift on the client phones, the client will contact the server on a periodic basis, using the Network Time Protocol (NTP), to give the server information about that specific phone's current clock readings. This permits the server to properly account for clock drift and synchronize the incoming signals with the server's high-precision clocks. This procedure is necessary to more accurately estimate the epicenter of an earthquake from probe measurements (Lawrence, Cochran et al 2008).

For events where clock synchronization is not available, cross correlation techniques may be used to properly shift the incoming time-signals. This process will also be necessary when analyzing the time domain properties of the signal, such as the Normalized Prediction Error or NPE (Baise, Glaser, 2000). Such parameters are indicators of the validity and noise-level of the transmitted signals.

3.4.4 iShake Map Generation

After aggregation and validation of the transmitted shakes, the iShake server can produce a contour map of the processed shakes. In a similar presentation to the Shake Maps developed by USGS (http://www.conservation.ca.gov/cgs/sm), iShake can produce a geospatially-varying intensity map from the filtered and processed accelerometer recordings of the iShake clients (e.g., Fig. 18). Once the server has validated and processed the required data, the summarized information can be visualized on the phones of the iShake users. This feature will not only serve as an immediate notification method for nearby earthquake events of interest, it will also provide the iShake users as well as emergency responders with a high-resolution, detailed map of the likely impacted areas immediately after an earthquake event.

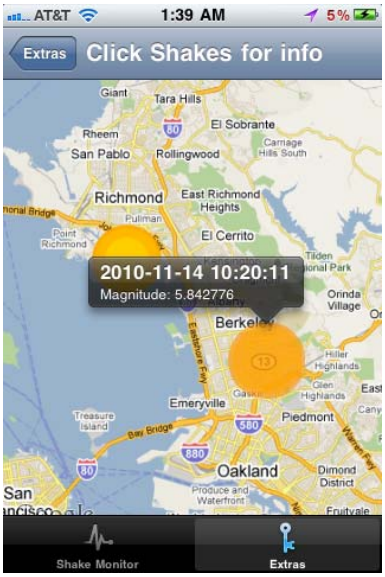

FIG. 18. Example of iShake Map Generated on Client Application from Test Event

4 FIELD TESTING

A comprehensive test plan and list of action items for the iShake field tests is described in the following sections. These tests are planned to be implemented in January of 2011 in the U.C. Berkeley campus. A chronological order of events, how the user study will be conducted, study objectives, field testing procedures, test participants, and data collection methodologies are described briefly in the following sections.

4.1 Objectives

Abowd et al. (2003) have pointed out that controlled studies in usability laboratories cannot lead to deep, empirical evaluation results. What is needed is real use in an authentic setting. Therefore, in order to gain as reliable understanding of user experience as possible, the user study will be implemented to investigate the users' experiences evoked by the iShake service. Factors that affect users' acceptance of the service are also examined.

In the study is pursued to identify the individual value parameters brought to the user through the application. Jurison (2000) has concluded that applications which are perceived to offer high value from the start are adopted rapidly while those perceived to be of low value are adopted slowly and are unlikely to gain acceptance in the long run. Our aim is to have the users to adopt the iShake into the long-term use and use it as a critical information channel in the case of an earthquake. Participative planning will also be organized with test users for designing and visioning how to iterate the iShake for future use.

Through the user study we want to obtain guidelines and requirements for iShake's future development and improvement. We want to better comprehend what kind of information and instructions users would want to receive from the iShake in the event of an earthquake. Our objective is to better understand iShake's possibilities for influencing people's lives especially on regions prone to earthquakes.

4.2 User Studies

Our goal is to most efficiently test the functionality and scalability of the iShake system and we want to gain the most profound understanding of the iShake users. Therefore, we aim to get as many volunteers to participate in field tests as possible. The iShake application will be made available for unrestricted downloading among the UC Berkeley community, which will be used as a recruiting pool for test participants.

According to Battarbee (2004) describing and understanding user experience is challenging as user experience is always multifaceted and difficult to verbalize and describe. Combining different data collection methods increases the reliability and validity of the user study results (Isomursu et al., 2007). Therefore, in the iShake user study we utilize a variety of data collection methods that are highly complementary (Yin, 2003).

With a focus group will be arranged a workshop to explore users' experiences and thoughts about the iShake. The workshop participants will be recruited among the iShake test users. The purpose is to plan with the users the future development and improvement of the iShake. In the workshop the users will create usage scenarios of the iShake. The scenarios will tell how the iShake influences people's lives by acting as the critical information channel during the earthquake. In the scenarios are described how a certain user type will use the iShake in a given context during the earthquake, and what kind of information and instructions in what format should the iShake provide to user. Scenario stories will be analyzed to get guidelines and input for the designers to develop the iShake further.

4.3 Test Plan and Schedule

A comprehensive pilot test will be implemented with around dozen people before introducing the application to the wider audience and releasing the app for users to download. Based on pilot test findings, possible modifications will be made to the iShake system accordingly.

After the pilot test, the application will be made available for downloading by the UC Berkeley community members. Field tests will begin at the UCB campus in the end of January 2011 as two separate test events. During the test events the users are asked to all shake their iPhones at the same time. The servers will collect the measurement data from the users' iPhones. All the users are also asked to fill in the related user study questionnaire via their iPhones. The measurement data collected from the field tests will be utilized to analyze the functionality of the technology, i.e. the sensing, transmission, and display capabilities of the iPhones. The analyzed data will be utilized to improve and develop the system further.

Muller et al. (2003) argue that in order for people to be able to reflect meaningfully on their experiences, they need time to do so, and if people are supposed to determine relevance and purpose of evaluated service through experimentation, they need even more time. In the case of field studies with a new service, the novelty effect may last several weeks. Therefore, after the field tests at the UCB campus, the users will have the iShake application in active everyday use during a two-week period, when the users are asked to continue using their iPhones (with installed iShake app) as usual. During the testing period we produce and deliver imaginary information about earthquakes to the users' iPhones via the iShake application. During this longer testing period we want to mimic the central idea and future use of the iShake where the users will be provided earthquake notifications by the application. The users will be asked to treat the earthquake information as it was authentic. During the testing period the users will record on mobile questionnaires their activities and context at the time of the "earthquake", as well as various dimensions of their subjective experience. We use real-time mobile questionnaires to assess user experiences at the time that they occur as the users are in natural settings.

4.3.1 Structure of testing

The general form for the field test will be the following:

1) Early warning
2) Very late warning
3) Actual earthquake alert
4) Notification about new earthquake data
5) Request to fill out questionnaire

All earthquake events during the field testing will follow exactly the above five-point structure, in addition to:

6) Nightly reminder to turn on the application at night and leave it on.

4.3.2 Recordings at Night

When phones are charged (for example at night when people are asleep), they are not being used and are in a resting position. This situation offers an opportunity for reliably sensing earthquakes, since during the charging time phones have unlimited power and they are stabilized.

Therefore, the phones are able to detect ground motions where they are without contamination of the signal by human motion. In consequence, iShake users are asked to simply turn on the application when they plug in their phone at night. Then any possible earthquake triggers measured by the phone will instantly be streamed back to iShake servers for further processing and shake map generation.

4.3.3 User-Generated Graphs

An iShake map will be generated on the users' phone showing the intensity of shaking obtained from the phones in the network. iShake users can select to view the information obtained from their own phone only or those obtained from other users. These real-time Shake Maps will instantly be available for viewing for the user on the application as well as on the iShake website. In addition, through the link referred to as the "iShake Signal Grapher" on the project website, the users can view online the accelerograms sent from their iPhones as well as the time and location of each record.

5 CONCLUSIONS

Emergency responders must "see" the effects of an earthquake clearly and rapidly so that they can respond effectively to the damage it has produced. Great strides have been made recently in developing methodologies that deliver rapid and accurate post-earthquake information. However, shortcomings still exist. The iShake project is an innovative use of cell phones and information technology to bridge the gap between the high quality, but sparse, ground motion instrument data that are used to help develop ShakeMap and the low quality, but large quantity, human observational data collected to construct a "Did You Feel It?" (DYFI)-based map.

The iShake project is using people's cellular smart phones to measure ground motion intensity parameters and automatically deliver the data to the U.S. Geological Survey (USGS) for processing and dissemination. In this participatory sensing paradigm, quantitative shaking data from numerous cellular phones will enable the USGS to produce shaking intensity maps more accurately than presently possible.

The phone sensor is an imperfect device with performance variations among phones of a given model as well as between models. The sensor is the entire phone, not just the micro-machined transducer inside. A series of 1-D and 3-D shaking table tests were performed at UC San Diego and UC Berkeley, respectively, to evaluate the performance of a class of cell phones. In these tests, seven iPhones and iPod Touch devices that were mounted at different orientations were subjected to 124 earthquake ground motions to characterize their response and reliability as seismic sensors. The testing also provided insight into the seismic response of unsecured and falling instruments.

Pilot software has been developed that captured the measured data during the shaking table tests. The data are sent automatically as a text message immediately after the shaking occurs (and before high cellular phone traffic blocks most cell phone use) to a server that can analyze and interpret the data.

The cell phones measured seismic parameters such as peak ground acceleration (*PGA*), peak ground velocity (*PGV*), peak ground displacement (*PGD*), and 5% damped spectral accelerations well. In general, iPhone and iPod Touch sensors slightly over-estimated ground motion energy (i.e., Arias Intensity, I_a). However, the mean acceleration response spectrum of the seven iPhones compared remarkably well with that of the reference high quality accelerometers. The error in the recorded intensity parameters was dependent on the characteristics of the input ground motion,

particularly its *PGA* and I_a, and decreased for stronger motions. The use of a high-friction device cover (e.g., rubber iPhone covers) on unsecured phones yielded substantially improved data by minimizing independent phone movement. Useful information on the ground motion characteristics was even extracted from unsecured phones during intense shaking events.

The insight gained from these experiments is valuable in distilling information from a large number of imperfect signals from phones that may not be rigidly connected to the ground. With these ubiquitous measurement devices, a more accurate and rapid portrayal of the damage distribution during an earthquake can be provided to emergency responders and to the public.

REFERENCES

Abowd, G. D., Mynatt, E. D., and Rodden, T. (2002). "The Human Experience." *IEEE Pervasive Computing*, Vol. 1, No. 1, IEEE Computer Society, pp. 48-57.

Abrahamson, N. A., Somerville, P. G., and Cornell, C. A. (1990). "Uncertainty in numerical strong motion predictions." *Proc. 4th U.S. Nat. Conf. on Earthquake Engrg.*, EERI, El Cerrito, Calif. 407-416

Baise, L.G., and Glaser, S.D. (2000). "Consistency of Ground-Motion Estimates Made using System Identification." *Bulletin of the Seismological Society of America*, 90, 4, pp. 993–1009.

Battarbee, K. (2004). "Co-experience: Understanding User Experience in Social Interaction." *Academic dissertation*. Publication series of the University of Art and Design Helsinki.

Black, H.D (1964). "A Passive System for Determining the Attitude of a Satellite." The Johns Hopkins Univ., *AIAA Journal*, 2(7).

Dankmar B Johning (1992). Multinomial logistic regression algorithm. Annals of the Institute of Statistical Mathematics, 44:197–200.

Dashti, S., Bray, J. D., Pestana, J. M., Riemer, M. R., and Wilson, D. (2010b) "Centrifuge Testing to Evaluate and Mitigate Liquefaction-Induced Building Settlement Mechanisms." *J. Geotech. Geoenviron. Eng.*, 136(7), 918–929.

Isomursu, M., Tähti, M., Väinämö, S., and Kuutti, K. (2007) "Experimental evaluation of five methods for collecting emotions in field settings with mobile applications." *International Journal of Human-Computer Studies*, Vol. 65, No. 4, Elsevier, pp. 404-418.

Joyner, W. B., and Boore, D. M. (1988). "Measurement characteristics and prediction of strong ground motion." State of the Art Rep., Proc. Spec. Conf. on Recent Adv. In Ground Motion Evaluation, ASCE, Reston, Va., 43-102

Jurison, J. (2000) "Perceived Value and Technology Adoption Across Four End User Groups." *Journal of Organizational and End User Computing*, Vol. 12, No. 4, IGI Global, pp. 21-28.

Lawrence, J. F.; Cochran, E. S.; Christensen, C.; Jakka, R. S. (2008), "Distributed Computing and MEMS Accelerometers: The Quake Catcher Network", *American Geophysical Union*, Fall Meeting 2008, abstract #IN23A-1068

Mason, H.B., Bray, J.D., Jones, K.C., Chen, Z-Q., Hutchinson, T.C., Trombetta, N.W., Choy, B.Y., Kutter, B.L., Fiegel, G.L., Montgomery, J., Patel, R.J., Reitherman, R., Bolisetti, C., and Whittaker, A.S., (2010) "Earthquake Input Motions and Seismic Site Response in a Centrifuge Test Examining SFSI Effects," Fifth International Conference on Recent Advances in Geotechnical Earthquake Engineering and Soil Dynamics, May 24-29, San Diego, CA, Paper No. 5.48a.

Muller, M. J., Raven, M. E., Kogan, S., Millen, D. R. and Carey, K. (2003). "Introducing Chat into Business Organizations: Toward an Instant Messaging Maturity Model." *The 2003 International SIGGROUP Conference on Supporting Group Work (GROUP 2003)*, Sanibel Island, Florida, USA, ACM Press, pp. 50-57.

Wald, D. J., Quitoriano V, T. H. Heaton, H. Kanamori, C. W. Scrivner, and C. B. Worden. Trinet (1999) "'shakemaps': Rapid Generation of Peak Ground Motion and Intensity Maps fFor Earthquakes in Southern California," EARTHQUAKE SPECTRA, 15(3):537–556.

Wong, I., Thomas, P., and Somerville, P. (2008). "Updated probabilistic seismic hazard evaluation and development of seismic design ground motions for the University of California, Berkeley and Lawrence Berkeley National Laboratory." Final Report Prepared by the URS Corporation.

Yin, R.K. (2003) *Case Study Research: Design and Methods*. Sage Publications, London, 3rd edition.

BIBLIOGRAPHY

[Publications produced by this research at the time of this report]

Dashti, S., Reilly, J., Bray, J.D., Bayen, A., Glaser, S. and Mari, E. (2010) "iShake: Mobile Phones as Seismic Sensors," American Geophysical Union Fall Meeting Abstract & Presentation, San Francisco, Dec. 17.

Dashti, S., Reilly, J., Bray, J.D., Bayen, A., Glaser, S. and Mari, E. (2011) "iShake: Using Personal Devices to Deliver Rapid Semi-Qualitative Earthquake Shaking Information," GeoEngineering Report, Depart. of Civil and Environ. Engineering, Univ. of California, Berkeley, Feb 28.